water

MDPI

Article

Hydropower Potential of Run of River Schemes in the Himalayas under Climate Change: A Case Study in the Dudh Koshi Basin of Nepal

Daniele Bocchiola [1,2,*], Mattia Manara [1] and Riccardo Mereu [3]

[1] Department of Civil and Environmental Engineering (DICA), Politecnico di Milano, L. da Vinci 32, 20133 Milano, Italy; mattiamanar@gmail.com
[2] EVK2CNR Committee of Italy, S. Bernardino 145, 24122 Bergamo, Italy
[3] Department of Energy Engineering (DENG), Politecnico di Milano, Campus-Bovisa, Lambruschini, 4a, 20156 Milano, Italy; riccardo.mereu@polimi.it
* Correspondence: daniele.bocchiola@polimi.it

Received: 20 July 2020; Accepted: 16 September 2020; Published: 19 September 2020

Abstract: In spite of the very large hydropower potential given from the melting snow and ice of Himalayas, Nepal's population has little hydropower production. The high use of fossil fuels and biomasses results in measurable air pollution, even in the mountain areas. Hydropower planning and implementation, in the face of the changing climate, is therefore paramount important. We focus here on Nepal, and particularly on the Dudh Koshi river basin, with a population of ca. 170,000 people, within an area with large potential for hydropower production. Our main objectives are to (i) preliminarily design a local hydropower grid based on a distributed run of river *ROR* scheme, and (ii) verify the resilience of the grid against modified hydrology under perspective climate change, until the end of the century. To do so, we set up and tune the *Poli-Hydro* semi-distributed glacio-hydrological model, mimicking the complex hydrology of the area. We then modify a state of the art algorithm to develop and exploit a heuristic, resource-demand based model, called *Poli-ROR*. We use *Poli-ROR* to assess the (optimal) distribution of a number of *ROR* hydropower stations along the river network, and the structure of the local mini-grids. We then use downscaled outputs from three general circulation models GCMs (RCPs 2.6, 4.5, 8.5) from the Intergovernmental Panel on Climate Change IPCC AR5, to assess the performance of the system under future modified hydrological conditions. We find that our proposed method is efficient in shaping *ROR* systems, with the target of the largest possible coverage (93%), and of the least price (0.068 € kWh^{-1} on average). We demonstrate also that under the projected hydrological regimes until 2100, worse conditions than now may occur, especially for plants with small drainage areas. Days with energy shortage may reach up to $n_f = 38$ per year on average (against $n_f = 24$ now), while the maximum daily energy deficit may reach as high as $e_{def\%} = 40\%$ (against $e_{def\%} = 20\%$ now). We demonstrate that our originally proposed method for *ROR* grid design may represent a major contribution towards the proper development of distributed hydropower production in the area. Our results may contribute to improve energy supply, and living conditions within the Dudh Koshi river. It is likely that our approach may be applied in Nepal generally. Impending climate change may require adaptation in time, including the use of other sources which are as clean as possible, to limit pollution. Our *Poli-ROR* method for grid optimization may be of use for water managers, and scientists with an interest in the design of optimal hydropower schemes in topographically complex catchments.

Keywords: mini-hydropower; hydrological modeling; Nepal; climate change

1. Introduction

The provision of secure and affordable energy is essential to fostering human development and economic growth. The bearing of safe access to energy upon sustainable development was recognized by the United Nations in September 2015, when 193 countries adopted the 2030 Agenda for Sustainable Development [1]. This was a set of 17 goals, aimed at ending poverty, protecting the planet and ensuring prosperity for everyone. Energy occupies a central place among the world's development priorities, as indicated in the sustainable development goal SDG 7, i.e., " ... *ensure access to affordable, reliable, sustainable, and modern energy for all.*" Despite the progress made in this direction, according to the International Energy Agency [2], 1060 million of people worldwide still lack access to electricity, 84% of whom live in rural areas. The difficulty of serving rural inhabitants lays in a combination of complex topography, and low population density, making extension of the main grid not economically viable [3]. Stand-alone and mini-grid systems, including those based upon run-of-river *ROR* plants, are gaining increasing attractiveness due to the declining cost of renewables, and more efficient end-user appliances. Technological changes are providing an opportunity to evolve and play a significant role in accelerating the pace of electrification [4].

With an estimated gross domestic product GDP of US$1071 per capita (2019), Nepal is ranked amongst the poorest countries worldwide, and (2010) 25% of the population earn below US$1.90 per day [5,6]. In spite of the large supply of freshwater from the melting snow and ice of the Himalayas [7,8], a large share of the population has no access to safe drinking water, food [9–11], and clean electricity [12,13]. It is estimated [14,15] that ca. 96% of the urban population has access to electricity, and 93% in rural areas. However, only 1–3% of energy demand is fulfilled via hydropower [16], and the lion's share is taken by wood burning (ca. 66%), and less by agricultural biomasses (ca. 15%, [17]). A large share is also given in rural areas by burning of dried animal dung (ca. 8%). Imported fossil fuels are present, albeit somewhat low (ca. 8%), with large pollution levels [18–21]. According to the most recent scenarios of the intergovernmental panel on climate change IPCC [11,17,22], in Nepal, temperatures in the next few decades may increase by +1 °C to +5–6 °C. Himalayan glaciers are shrinking, and will further shrink in the future [23], with a decrease in available water resources [24], for agriculture [25], and energy production [26–28]. Nepal is particularly susceptible to climate change [29–37], and the country has low adaptive capacity to respond to climate variability [38,39]. The economy largely leans on mountain tourism, and the yearly income from the tourism industry is reported to be over $360 million. A recent assessment of the hydropower potential indicated ca. 40–60 GW [12,15,40] in potential, but hitherto no more than ca. 800 MW is exploited, mostly using *ROR* plants [41] with little or no storage, and therefore subjected to flow seasonality and, possibly, climate changes. While the evaluation of site-specific hydropower potential was pursued in the area [41], an optimal, hydro-climatically based *ROR* scheme assessment strategy for a region or a certain watershed was not investigated. The reasons for this may be three-fold. Automatic (or semi-automatic) optimization algorithms for hydropower schemes were not specifically developed that we know of in the area, or worldwide, at least for catchments with complex topographic settings, and accordingly design is based upon subjective design, and educated guess. Information which is as accurate as possible is required about the magnitude and seasonality of stream flows, which are also distributed in space, and may be attained with accurate, data-rich hydrological modelling (or via distributed flow monitoring, however expensive, and complex in such high altitude areas). Moreover, the assessment of future hydropower potential under climate scenarios (of the Intergovernmental Panel on Climate Change IPCC) needs specific scenarios of future hydrology. The development of such scenarios require complex hydrological modeling, especially at high altitudes and cryospheric driven catchments.

We focus here on studying one such *ROR* system for the Dudh Koshi catchment of Nepal. Dudh Koshi (Solokhumbu district, see, e.g., [22,42]), is the gateway to Everest, and nests the iconic Khumbu glacier, and it is visited every year by plenty of tourists. However, the food security of the locals is at stake [43,44], as a result of population growth and climate change. Access to electricity is erratic, and almost totally based on the burning of biomasses, with subsequently high levels of

pollution [45]. The population in the Dudh Koshi catchment, covering the Solu Khumbu district and part of the Khotang district [25], was estimated to be ca. 170,000 persons as of 2011 [46], and is expected to rise to ca. 230,000 in 2050, with a tenfold density at the lowest altitudes. According to recent studies [47], the Koshi river displays a large risk of water scarcity under climate change, and population increase. Accordingly, one needs to plan for developing, clean, safe electric power systems. A project for design of a large hydropower plant catching water from the Dudh Koshi slightly downstream Rabuwa Bazar started in 1998; it is still ongoing [48], albeit lagging behind, and in our knowledge no large hydropower installation is presently in the catchment. One thus needs to explore other solutions, including *ROR* types of plants, and distribution via local mini-grids. This study aims at (i) providing a template for planning (optimal) off-grid rural electrification with *ROR* plants, based upon hydrological knowledge, and (ii) assessing the climate resilience of the system, under modified hydrology throughout the XXI century.

We first set up and tuned the *Poli-Hydro* semi-distributed hydrological [22,49], which can depict the complex, cryospheric driven hydrology of the Dudh Koshi river. We subsequently estimated the energy demand of the inhabitants within the boundary of the catchment, and of their limited economic activities (agriculture and tourism). We then developed a module *Poli-ROR*, which can be used to analyze various possible electrification schemes, including number, position, and hydropower potential of the *ROR* plants along the river network. *Poli-ROR* applies an appropriate heuristic algorithm, that produces objective scores, and helps the retrieval of an (economically) optimal *ROR* configuration from among the possible ones. Then, to assess future climate conditions, we properly downscaled temperature and precipitation projections by three general circulation models GCMs (EC-EARTH, ECHAM6, CCSM4) under three climate scenarios (RCP 2.6, 4.5, 8.5). We subsequently used these scenarios as inputs to *Poli-Hydro*, to evaluate the impacts upon catchment hydrology. *Poli-ROR* was then run under potentially modified hydrological scenarios, to assess the *ROR* system performance at mid-century (2041–2050), and end of century (2091–2100).

2. Case Study Area

The Dudh Koshi river (Figure 1) lies in the mid-hills of the central Nepal, located about 100 km East of Kathmandu (the capital city), and is one of the seven sub basins of the Sapta Koshi. Dudh Koshi is watered by snow and ice melt from above, including the Khumbu glacier, and is undergoing a reduction in stream flows in response to climate change and glacier area reduction [22,50]. The Dudh Koshi River upstream of Rabuwa Bazar has 90 km in length, and a catchment area of ca. 3600 km^2, one third of it above 5000 m a.s.l. Glaciers are present between 4900 and 7500 m a.s.l., mostly from 4800 to 6000 m a.s.l. The ice covered area is ca. 25% of the total area. The climate ranges from subtropical to polar [51], and the topography is rugged, with occasional plateaus where farming is carried out. Recent findings [52] for the Indrawati basin, ca. 100 km East of Dudh Koshi, indicated that the water poverty index WPI [31,53] was ~52.5 out of 100 (i.e., medium poor), and access to water is a major issue. The population of the area is therefore at large risk of severe impacts from changes in temperature and precipitation patterns [1,5,54]. Energy wise, the population in the Dudh Koshi area largely relies upon wood burning, kerosene, agricultural biomasses, and burning of animal dung at the highest altitudes. The local population has built a famously successful mountain tourism industry, and religious centers, handicraft production, trekking tourism, apple and potato agriculture, animal husbandry, and other livelihood practices, that are widespread for Sherpa, Rai, Limbu, Magar, Tamang, Tibetan, and other local populations.

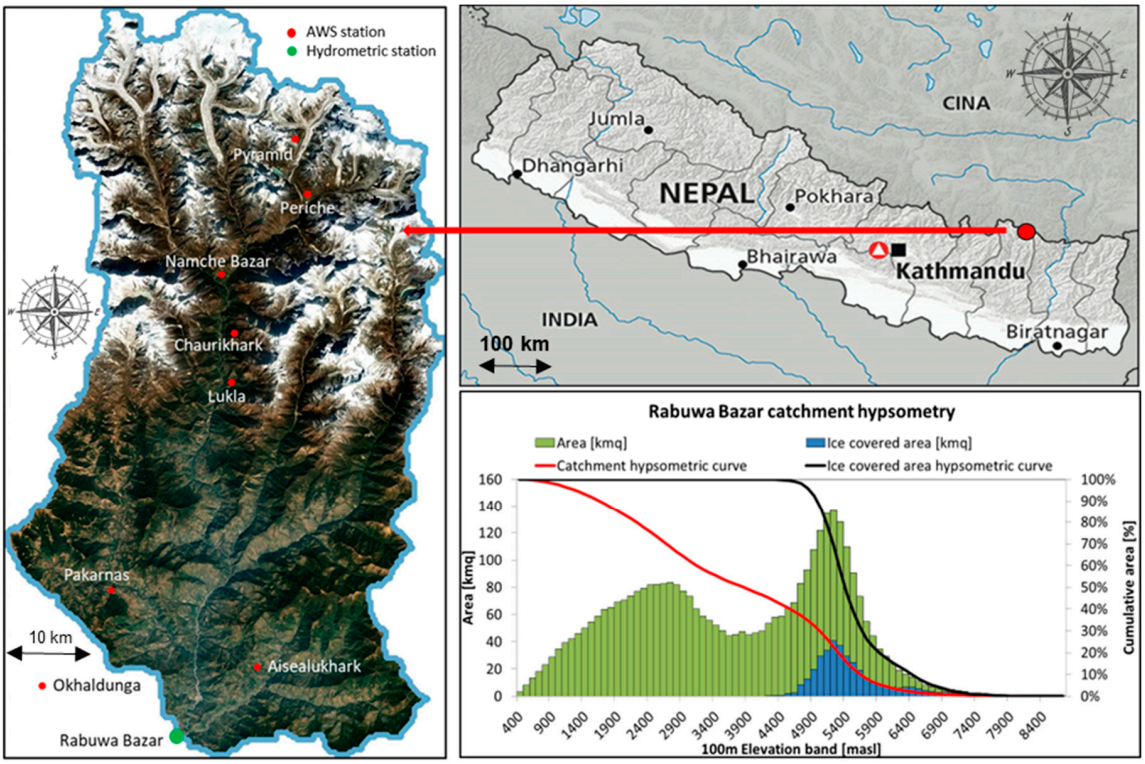

Figure 1. Case study area. Dudh Koshi basin location, and topography. Weather and hydro stations used in the study are reported. AWS = Automatic Weather Station. Topography was extracted from ASTER GDEM, resampled at 300 m × 300 m.

3. Data Base

3.1. Topography, Land Use, and Hydrological Data

The hydrological model *Poli-Hydro* requires as input spatial data of the basin (altitude, ice-cover, and land use), and meteorological data (temperature, precipitation). Spatial inputs, such as the fraction of vegetated soil f_v, maximum soil water content S_{max}, and digital elevation model of the area (DEM, here ASTER GDEM) are required. These data were derived from public thematic maps, and aggregated to obtain regular square cells of 300 m × 300 m side. The curve number *CN* map was estimated by cross-referencing the land cover map provided by the International Center for Integrated Mountain Development ICIMOD [55], and the Soil and Terrain database for Nepal developed by FAO [44,56]. Soil cover data were also used for creating the map of the vegetated soil fraction [33,43].

The *Poli-Hydro* model requires (daily) inputs of total precipitation *P*, snow depth *HS* whenever available, temperature *T*, and values of instream flows *Q* for calibration/validation purposes. In Table 1, we report the measuring stations, and hydro-climatic variables used here.

Remote sensing information was gathered to depict complex precipitation distribution within the catchment [22,57,58]. Namely, we used precipitation estimates from the tropical rainfall measuring mission TRMM (e.g., [59]). We used data from the 2B31 product, combined Precipitation Radar (PR)/TRMM Microwave Imager (TMI) rain-rate product, with path-integrated attenuation at 4 km horizontal, and 250 m vertical resolutions, processed by Bookhagen [60], and averaged over 12 years (1998–2005). In spite of displaying large overestimation of precipitation in the high altitudes (*Alt* > 3000 m a.s.l. or so), especially during winter (shown in [14]), TRMM estimates depict spatial distribution patterns of precipitation, not visible when using the (few) ground stations as here (see e.g., [61] for a similar issue in the Andes of Chile).

Table 1. Hydro-climate stations used in the study. DHM is the Nepal Department of Hydro-Meteorology. EvK2-CNR is EvK2-CNR committee of Bergamo, Italy. *T* is temperature, *P* precipitation, *HS* is snow depth, *Q* is stream flow.

Station	Alt [m a.s.l.]	Variable	Period	Resolution	Data Source
Okhaldunga	1720	*T*	1996–2013	daily	DHM
Lukla	2660	*T*	2003–2013	hourly	EvK2-CNR
Namche	3570	*T*, *P*	2003–2013	hourly	EvK2-CNR
Periche	4260	*T*, *P*	2003–2013	hourly	EvK2-CNR
Pyramid	5035	*T*, *P*, *HS*	2003–2013	hourly	EvK2-CNR
Aisealukhark	1924	*P*	1970–2013	daily	DHM
Pakarnas	2231	*P*	1970–2013	daily	DHM
Chaurikhark	2619	*P*	1970–2013	daily	DHM
Rabuwa Bazar	480	*Q*	2003–2013	daily	DHM

3.2. Demographic Data

The *Poli-ROR* model requires data of population, and their distribution. The demographic distribution was estimated from census of the government of Nepal, which was then spatialized with the aid of datasets coming from international organizations. The last census dates back to 2011 [46]. Nepal-wide data were integrated by using the location of the largest settlements nested into the basin [62], and a grid map of estimated population distribution [63]. We used the *Worldpop* data, which provide disaggregate country census data [64]. Prior to the use in population estimation, the *Worldpop* map was rescaled to match the model's resolution.

4. Methods

4.1. Hydrological Model

We used here the *Poli-Hydro* model. This is a physically based, semi-distributed glacio-hydrological model, validated previously [25,65] with acceptable performance, including within the Dudh Koshi catchment [66]. *Poli-Hydro* tracks water budget in soil between two consecutive days, taking as input liquid precipitation (rainfall) R, and ice/snow melt, M_l/M_S. Melt is calculated using a hybrid degree day model [67], considering temperature T, and (global, topographically corrected) solar radiation G.

Poli-Hydro can also track glaciers' flow, necessary for long term assessment of climate change impact [25,61]. Initial ice thickness $h_{ice,in}$ on glaciers is strongly influenced by the superficial slope (i.e., the greater the slope, the thinner the ice). We estimated $h_{ice,in}$ as described by Oerlemans [68], by back calculation from the basal shear stress τ_b (Pa). We assessed basal shear as a function of glacier's altitude jump ΔH as in Haeberli and Hoelzle [69]. Hydrological response is modeled via Nash model [70], with lag time $t_{l,s,g} = n_{s,g}\, l_{s,g}$, i.e., for $n_{s,g}$ reservoirs (here, $n_{s,g} = 3$) each with lag time $l_{s,g}$, for overland flow, and subsurface flow, respectively (s, and g subscript). Once calibrated against observed stream flows, *Poli-Hydro* provides stream flow estimates within any section along the river network, and such estimates can be used for assessment of hydropower potential, as if they were (virtual) hydrometric stations. In Table 2, we report *Poli-Hydro* model main parameters [71], including calibration method, whenever required.

The model is well described elsewhere, and we provide here a short description using the flow chart in Figure 2a [49,67]. The modeling procedure, and tools are therein given according to 7 categories. These are, namely domain of investigation (e.g., hydrology, cryosphere), tools (e.g., hydrological model, snow melt model, etc.), functions linking variables (e.g., snow melt M_s as a function of temperature, and radiation $M_s(T, G)$, etc.), necessary field surveys (ice melt from stakes, etc.), network data (of weather, snow depth, SCA from remote sensing, etc.), model outputs (e.g., ice melt in time at different time and place M_i(t,s)), and model accuracy (i.e., objective measure of matching against observed stream flows).

Moreover, in the flow chart the procedure to develop hydrological projections is reported. We also give the information necessary to model each component, and the interactions between components. Specific implementation of the proposed method clearly requires tailoring for each case study, and depends upon the characteristics of the area, and the available data and tools.

Table 2. *Poli-Hydro* model parameters, and corresponding values. In **bold**, calibration parameters.

Parameter	Description	Value	Method
T_s (°C)	rainfall/snowfall threshold	0	literature
DDF_s (mm day^{-1} °C^{-1})	degree day factor snow	3.5	snow depth data
DDF_i (mm day^{-1} °C^{-1})	degree day factor ice	2.5	snow depth data
SRF_s (mm day^{-1} W^{-1} vm^2)	radiation factor snow	6.5×10^{-3}	snow depth data
SRF_i (mm day^{-1} W^{-1} vm^2)	radiation factor ice	3.5×10^{-3}	snow depth data
α_s	albedo snow	0.7	radiation data
α_i	albedo ice	0.4	radiation data
K [mm day^{-1}]	soil transmissivity as saturation	1	monthly flows volumes
k_g	soil transmissivity exponent	2	monthly flows volumes
θ_w	water content wilting	0.15	literature
θ_l	water content field capacity	0.35	literature
θ_s	water content saturation	0.45	literature
$t_{l,s}$ (h)	lag time, surface	240	stream flows, timing
$t_{l,g}$ (h)	lag time, subsurface	1200	stream flows, timing

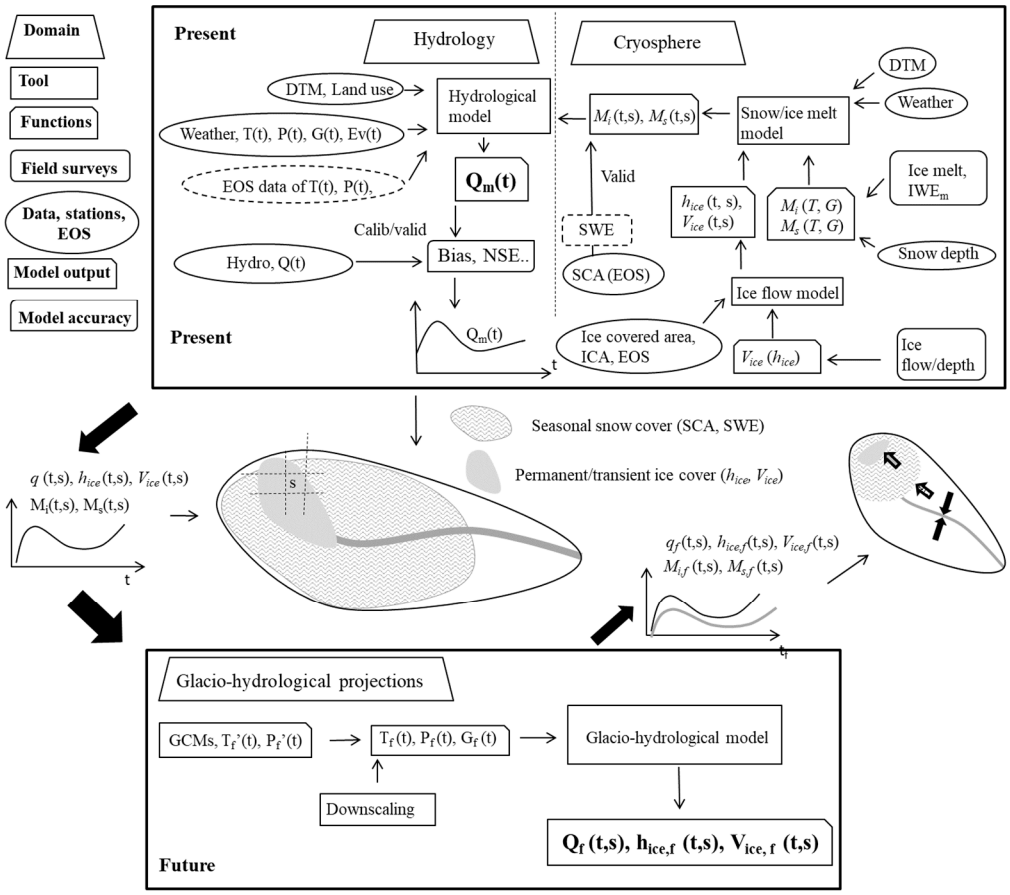

(**a**)

Figure 2. *Cont.*

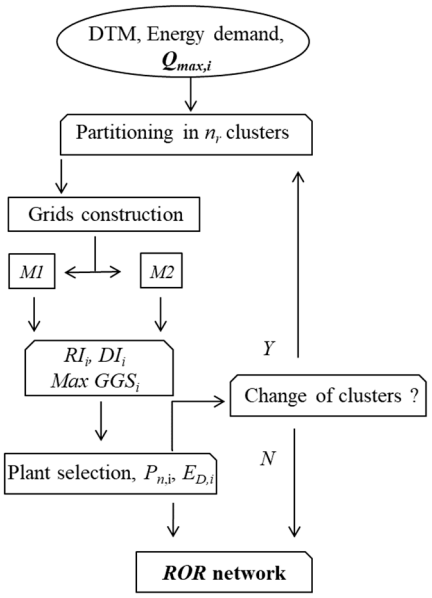

(**b**)

Figure 2. Flow chart (**a**) *Poli-Hydro* model. The modeling procedure, and tools are given according to 7 categories, i.e., domain (e.g., hydrology, cryosphere), tools (e.g., hydrological model, snow melt model), functions (e.g., snow melt M_s as a function of temperature, and radiation $M_s(T, G)$, etc.), necessary data from field surveys or other sources (ice melt from stakes, ice volume loss from topographic methods, earth observation from space *EOS*, etc.), data (weather, snow depth, SCA from remote sensing, etc.), model outputs (e.g., ice melt in time and space $M_i(t,s)$), and model accuracy (e.g., Bias, NSE). Division in present, and future (projections) reported. Dashed lines indicate methods/data that could be used generally as alternatives in high altitude catchments, but were not used here (e.g., snow depth data were not available, etc.). In **bold,** most important model outputs. $T(t)$ is daily temperature, $P(t)$ daily precipitation, $Q(t)$ is daily observed discharge at the outlet section, $Q_m(t)$ is daily modeled discharge at the outlet section. M_i(t,s) is daily ice melt in a given place (cell) s, $M_s(t,s)$ is daily snow melt, q(t,s) is daily runoff in cell s, h_{ice}(t,s) is daily ice depth, and V_{ice}(t,s) daily ice flow velocity. SCA is the snow covered area. SWE is the snow water equivalent. ICA is the ice covered area, IWE_m is the water equivalent of ice melt. NSE is the Nash–Sutcliffe efficiency. DTM is the digital terrain model. $T_f'(t)$, $P_f'(t)$ are (future/projected) the temperature and precipitation from GCMs before downscaling (biased); T_f (t), P_f (t) future daily temperature and precipitation after downscaling (unbiased). Q_f (t) future projected discharges. (**b**) *Poli-ROR* iterative algorithm. *Poli-ROR* takes as input DEM, energy demand, and $Q_{max,I}$ calculated at each site i using outputs from *Poli-Hydro* (Section 4.3). *Poli-ROR* is performed by (i) area subdivision, or clustering, with the number of clusters giving the number of plants, and (ii) mini-grid construction, repeated iteratively until convergence (Section 4.5). *M1* is *Min-LCOE* approach, *M2* is *Max-Connection* approach. GGS_i is grid generation score at each cluster/plant (Equation (8)), DI_i demand indicator (Equation (9)), and RI_i resource indicator (Equation (11)) thereby. $P_{n,i}$ is power at each cluster/plant i (Equation (2)), and $E_{D,i}$ energy demand thereby (Equation (3)).

4.2. Energy Demand

Evaluation of energy demand was carried out according to three main sectors, namely (i) agriculture, (ii) residential, and (iii) tourism. Agricultural consumption was evaluated using the national energy consumption data given by the International Energy Agency IEA [2,72], in all villages identified as agricultural according to land cover analysis [43]. Due to differences of the living standards between rural and urban population, in the residential and tourist area, energy demand estimates (in Table 3) were made based upon a former study pursued in the upper part of the catchment [73]. These values were then refined considering a conversion from biomass fired heating

systems, to electricity-powered ones. This assumption is acceptable, since the energy demand of the inhabitants of the Dudh Koshi basin is extremely low compared to the hydroelectric potential of the area. Corrections were carried out considering the typical energy usage distribution among different sectors in the upper basin [74]. For tourism, energy demand was evaluated according to the tourist record provided by the Sagarmatha National Park Office, giving the number of tourists in each season. It was assumed that tourists were homogeneously distributed within the available lodges in the area. The location of the main lodges was provided by ICIMOD [75], providing information of the local energy demand. The tourist volume is higher from September to December and from March to May. The monsoon season (viz. the season with highest rainfall, and flows), and winter record very few tourists instead due to adverse climatic conditions. Thus, the former group of months was categorized as "trekking season" while the latter one as "rest of the year".

Table 3. Energy demand of different household types, as per household HH. Adapted from Proietti et al. [73].

Household Type	Energy Demand (kWh day^{-1} HH^{-1})	Lighting (%)	Cooking (%)	Other (%)
Residential	5.6	9	89	2
Lodge (trekking season)	11	9	89	2
Lodge (rest of year)	3.3	8	90	2

4.3. Plants' Design

Concerning water availability, we analyzed the typical yearly flow pattern at Rabuwa Bazar. Therein, one has a monsoonal season, with high flow rates and high variability, and a dry season with low, almost constant flows. Due to such seasonal effects, the maximum nominal flow of turbines must be close to the minimum site value. For this reason, the maximum nominal flow at a given site i was taken as

$$Q_{max,i} = \frac{\sum_{y=1}^{N_y} Q_{335,i}}{N_y} - EF_i \quad (1)$$

with N_y years of simulation, and $Q_{335,i}$ (m^3 s^{-1}) flow rate exceeded for 335 days in a year at site i, and EF_i environmental flow as site i. The value of the environmental flow was fixed at 10% of the minimum mean monthly discharge, according to the Nepalese regulation.

We considered as initial potential sites for a hydropower plant, those that satisfied three criteria. These criteria were (i) minimum area, i.e., a drainage area at the inlet point greater than 20 km^2, to ensure a sufficient flow availability; (ii) minimum head, i.e., value of gross (before hydraulic losses) head compatible with the operating range of the chosen turbines (only impulse turbines were taken into account, due to the high slopes that characterize the study area); and (iii) maximum distance between the inlet and outlet of 1 km, to avoid excessive penstocks' length. For each of site, a nominal discharge Q_n is chosen, to satisfy the daily energy demand of the closest village, i.e.,

$$P_n = \rho_w g Q_n \Delta H_{net} \eta_{hydr} \eta_{el} \eta_{mec} \quad (2)$$

$$E_D = \int_0^T P_n(t) dt \quad (3)$$

Therein, ΔH_{net} (m) is the net head, ρ_w (ca. 1000 kg m^{-3}) is water density, g (m s^{-2}) is gravity acceleration, and η_{hydr}, η_{el} and η_{mec}, are the hydraulic, electric and mechanic efficiencies, respectively. Instant power $P_n(t)$ (kW) is integrated over time to give an energy production covering for energy demand E_D (kWh) over a certain period T.

The network is then iteratively modified. At each time step, the grid is extended, by connecting the demand point to the closest node of the network built at the former step, and by increasing the

value of Q_n to account for the energy demand of the whole grid. The maximum workable flow $Q_{max,i}$ is selected as in Equation (1). Penstocks' diameters are computed, to reduce head losses below a certain percentage $e_{\%}$ of the gross head, and then rounded up according to commercial values:

$$\Delta H_{net} = \Delta H_{gross}(1 - e_{\%}) \tag{4}$$

The electrical network is designed considering a distribution connecting the demand points belonging to the same mini-grid, and a transmission network connecting the individual houses inside each demand point. We chose to use medium-voltage (33 kV), considering the minimum linear distance, and the altitudinal difference between starting and ending points. A constrain of maximum length for each route was introduced, to limit voltage drops and an excessive ramification of the mini-grids. To evaluate the length of the transmission network L_N, assumed to be in low-voltage (0.2 kV), it was hypothesized an evenly space distribution of the households inside the village

$$A_{HH} = A_{Vi}/NH;\ L_N = \sqrt{A_{HH}/\pi}(NH - 1) \tag{5}$$

where A_{Vi} is the area of each village, A_{HH} the area of influence assigned to each household, and NH the number of households in the village.

4.4. Cost Estimation

Grid cost assessment is carried out considering two mini-grids' components, namely (i) the hydroelectric plant, and (ii) the electrical network. The plant cost is thus estimated considering the average distribution of investment on a generic small hydropower plant [76], as reported in Figure 3. The cost of the turbo-generator set is computed using an empirical equation, specific for impulse turbines [76]

$$c_{turb} = 17.7 P_n^{-0.36} \Delta H_{net}^{-0.28} \tag{6}$$

where c_{turb} is the specific cost in EUR(kWh)$^{-1}$ of the group, turbine + alternator. The cost of the penstocks is derived from the same commercial tables used for the evaluation of the diameters. Finally, the total cost of the plant is derived giving to the penstock half share of the civil works cost. The costs of the electrical network are calculated, using the indications by IEA [3]. Finally, the levelized cost of the electricity *LCOE* is derived, and used in the subsequent procedure

$$LCOE = \sum_{t=1}^{n} I_t + OM_t/(1+r)^t / \sum_{t=1}^{n} E_t/(1+r)^t \tag{7}$$

where I_t are the investment costs at year t; OM_t the operational and maintenance costs; E_t the energy consumed yearly; with r discount rate.

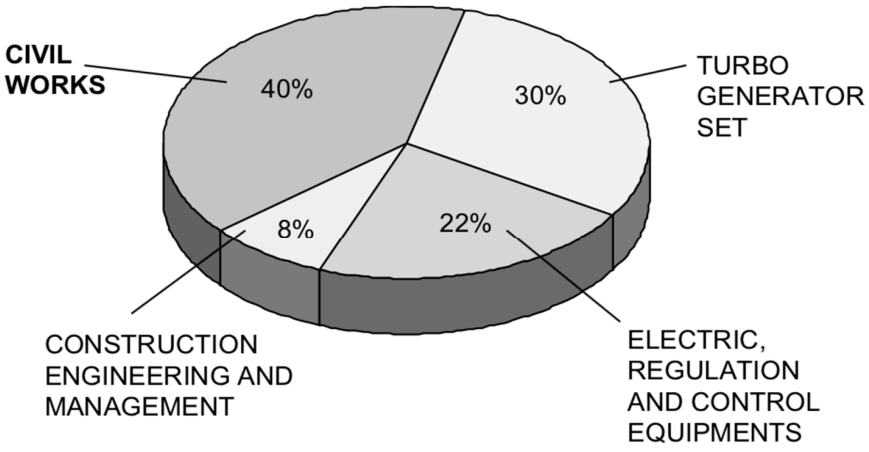

Figure 3. Average distribution of investment on a generic small hydro-power plant. Adapted from [76].

4.5. Heuristic Network Design Procedure, Poli-ROR

When dealing with decentralized energy network design at a regional scale as we are here, exact design procedures are rarely suitable, since they require introduction of questionable simplifications, and/or large computational times [65,77]. Here we chose to adopt a heuristic approach, adapted from a method introduced recently [78–80] to design mini-grids, powered by solar and wind energy. The method is suitable, because (i) the design procedure here is quite complex, and highly non-linear, and thus not suitable for classical approaches (e.g., linear programming), and (ii) the procedure allows to include a detailed description of the physical system involved, i.e., the hydrological, and hydroelectric set up of the area.

We developed a heuristic procedure, which we call *Poli-ROR*, based on a set of former heuristic indicators, proposed to support off-grid electrification projects [78]. Namely, we used (i) a resource indicator (hereon *RI*), that evaluates the economic convenience of producing energy from a specific plant, as compared to those located nearby, and (ii) a demand indicator (hereon *DI*) that evaluates the energy demand concentration at a given production point.

These two indicators are calculated, and then normalized (0–1) for every potential plant. Their value is then weighted by a parameter α (0–1), quantifying their relative importance, to obtain the suitability of a given point (stream section) I, to act as a production point for the mini-grid

$$GGS_i = \alpha RI_i + (1-\alpha)DI_i \tag{8}$$

The grid generation score *GGS* is computed for each plant. The purpose of the heuristic indicators is to identify the most promising pairs, or coupled points of inlet and outlet, for the implementation of a mini-grid. To be identified as an attractive generation point, a plant should (i) display a high energy demand concentration to serve a large number of users (high *DI*), and (ii) exploit water resources efficiently, i.e., to be more economically convenient against surrounding points (high *RI*). The initial demand indicator for a possible production point i, DI_i^0 is calculated by considering the set of N_i closest demand points, and by weighting the influence of each of them by their distance from the plant location

$$DI_i^0 = \sum_{j=1}^{N_i} \frac{ED_j}{\max\left(dist_{i,j}, L_{min}\right)} \tag{9}$$

with ED_j being the energy demand of the village j. A least distance L_{min} was set to avoid a null denominator in case of points belonging to the same cell. While the definition of *DI* is somewhat straightforward, finding a suitable *Resource Indicator RI* is more complex. In facts, the most appropriate way to compare two different couples in terms of economical convenience would be by *LCOE*. However, for a single plant *LCOE* is not fixed a priori, but it is a function of the number of villages thereby connected. Therefore, to compare different plants/couples it was decided to assign to each one a unique value, chosen as the average *LCOE* for a fixed number of connected villages to that plant n_i.

$$PI_i = \frac{\sum_{k=1}^{n_i} \frac{1}{LCOE_k}}{n_i} \tag{10}$$

with PI_i Potential Indicator for the plant i. Then, the initial Resource Indicator RI^0 is defined in analogy to DI^0 as

$$RI_i^0 = \sum_{j=1}^{N_p} \frac{PI_i - PI_j}{\max\left(dist_{i,j}, L_{min}\right)} \tag{11}$$

where PI_j are the values of the Potential Indicator of the N_p plants located closer to the plant j.

The *Poli-ROR* heuristic procedure is performed according to two steps, namely by (i) area subdivision, or clustering, and (ii) mini-grid construction. The procedure is iteratively repeated until convergence is reached, as shown in Figure 2b.

First, the study area is partitioned into a number n_r of sub-regions. Then in any sub-region, a possible generation point is selected, and a tentative mini-grid is constructed. During the construction phase, only demand points belonging to each sub-region are considered. The initial subdivision in sub-regions is then updated iteratively. The first/initial subdivision is carried out by applying a *k*-means clustering algorithm on the villages' geographical location, defining n_r centroids (one for each region), and their relative sub-area of influence, each sub-area being identified by assigning each point of the space to the closest centroid.

In the subsequent iterations, since for each cluster a tentative mini-grid will be defined in the second step, the centroid location is modified to match the tentative plant location, and the sub-areas are subsequently re-evaluated. It is implicitly assumed that each village will be connected to the closest plant. The clustering procedure has five steps, i.e., (i) randomly choose *k* initial cluster (centroids), (ii) compute the distance from each point to each centroid, (iii) assign each point to the cluster with the closest centroid, (iv) recalculate *k* new centroids as centers of mass of the clusters resulting from the mini grid construction step, and (v) repeat points 1–4 until the centroid position does not change any more.

In the grid construction step, inside each sub-area the plant with the highest value of *GGS* in Equation (8) is selected, and the mini-grid is designed as explained in Section 4.3. Two possibly contrasting objectives need to be taken into account, namely (i) maximizing the share of inhabitants served, and (ii) minimizing the average *LCOE* of the mini-grid. Based upon which objective is seen as more relevant, two different approaches can be pursued.

First, the *Min-LCOE* approach can be used, hereon method *M1*. This includes the selection of a grid set up with the lowest local value of *LCOE* for each mini-grid. In this approach, the *DI* and *RI* indicators are evaluated by selecting a number of demand points N_i, leading close to the average minimum *LCOE* value for all the different plants/couples.

Second, the *Max-Connection* approach can be used, hereon method *M2*. Here, the two indicators *DI* and *RI* are evaluated, selecting as a number of surrounding points N_i the maximum value for each pair.

The outcome of the heuristic optimization depends upon the values of three main parameters, namely the number of clusters (sub-regions) n_r, the maximum length of the transmission line between two villages L_{max}, and the weighting factor in Equation (8). To investigate such dependence, a sensitivity analysis was carried out. In Table 4, we report a resume of the *Poli-ROR* parameters, including their values, and those parameters that underwent a sensitivity analysis. After a preliminary screening, the hypothesis of adopting an electrical storage system (i.e., batteries) was deemed unfeasible, given the potentially required storage (i.e., size of batteries), and infrequent (i.e., few days per year) use of the storage. We thus assume that during dry days some plants will not be able to fully meet the energy demand of the inhabitants served, which will have to rely upon other energy sources (e.g., kerosene fed generators).

4.6. Future Scenarios

After having selected the best *ROR* scheme, the performances therein were evaluated under potentially changed future climate/hydrological conditions. The streamflow projections for the Dudh Koshi river were assessed by giving them as an input to *Poli-Hydro* temperature and precipitation projections. These were obtained by properly downscaling [81] the outputs of three GCMs, provided under the umbrella of the fifth coupled model intercomparison project CMIP5 (see Figure 2a). We considered three GCMs, namely ECHAM6 (European Centre Hamburg Model, version 6, [82]), CCSM4 (Community Climate System Model, version 4, [83]), and EC-Earth (European Consortium Earth system model, version 2.3, [84]), under three Representative Concentration Pathways scenarios (RCP 2.6, 4.5 and 8.5). Specifically, for each mini-grid we analyzed two indicators, i.e., the average

number of days per year with daily energy supply below the demand (system failure) n_f, and the maximum daily energy deficit in one year (e_{def}), which we used to benchmark the future performances against the present ones.

Table 4. Hydroelectric input parameters for *Poli-ROR*, and values assigned. SA means that a sensitivity analysis was carried out to assign a best value, see Section 4.5.

Parameter	Description	Value
$L_{penstock,max}$ (m)	maximum penstock length	1000
$A_{threshold}$ (km^2)	minimum catchment area	20
$P_{nom,max}$ (kW)	max maximum nominal power	1500
ED_{agr} (kWh ab^{-1} day^{-1})	agricultural energy demand	0.11
ED_{res} (kWh HH^{-1} day^{-1})	residential energy demand	8.25
$ED_{lodge,trek}$ (kWh HH^{-1} day^{-1})	trek lodges energy demand (trekking season)	16.2
$ED_{lodge,winter}$ (kWh HH^{-1} day^{-1})	winter lodges energy demand (winter season)	9.36
$e_{\%}$ (%)	maximum head loss (%) 5	5
c_{trans} (€ m^{-1})	transmission line cost	9
c_{distr} (€ m^{-1})	distribution line cost	5
$c_{conn,HH}$ (€ HH^{-1})	cost for connecting a household	100
c_{transf} (€ kV A^{-1})	transformers' cost	100
c_{batt} battery cost (€ unit^{-1})	battery cost	500
$Capacity_{batt}$ (Ah unit^{-1})	battery capacity	225
V_{batt} (V)	battery voltage	12
ele_{loss} (%)	transmission and distribution losses	5
r (%)	discount rate (%)	5
L_{max} (m)	maximum transmission length	SA
$n_{clusters}$	number of clusters	SA
α	weighting factors, *RI*, *DI*	SA

5. Results

5.1. Poli-Hydro Model

Table 5 and Figure 4 report the performance of the *Poli-Hydro* model. The parameters governing ice and snow melt (degree day, and the radiation factors, see Table 2) were calibrated against snow data (Table 1, see also [71]). Tuning of the hydrological parameters was pursued against the observed discharge at Rabuwa Bazar (see the calibration method in Table 2). We used monthly flow averages for K, and k_g regulating flow volumes, and daily flows for lag times, $t_{l,s}$, $t_{l,g}$. The entire period of simulation was subdivided into calibration *CAL* (2003–2007), and validation *VAL* (2008–2013) subsets, and the year 2009 was not used due to lack of observed data. We used three indicators, namely *Bias* (average percentage error), *NSE* (Nash–Sutcliffe Efficiency, or explained variance) ln_{NSE} (*NSE* of logarithmic values), given in Table 5. In calibration, *Poli-Hydro* overestimates the monthly cumulative discharge by *Bias* = +7%, and in validation it underestimates by *Bias* = −12%. On an annual basis, calibration would lead to *Bias* = +16%, while in the validation one has *Bias* = 0%, and *NSE* = 0.71, 0.66, respectively. Analysis of the flow contributions (not shown, see e.g., [85]) demonstrated that stream flows at Rabuwa bazar are mainly given by rainfall (ca. 69% of the yearly flows), and groundwater flow (ca. 23%), and overland flow from ice and snow melt is marginal (conversely to flow in the highest altitudes, see [71]). Clearly, a largest contribution is given during monsoonal season, displaying heavy precipitation, and highest temperature (i.e., larger snow and ice melt). In Figure 4, we report model adaptation. Therein, the model visibly reproduces poorly peak discharge. Notice that *Poli-Hydro* model is not designed to reproduce high flows, say for flood assessment, also given its daily resolution, and such exercise clearly requires other methods.

Table 5. Model efficiency in calibration and validation periods. Indicators explained in Section 5.1.

Indicator Period	*Bias* Monthly (%)	*Bias* Year (%)	*NSE* Daily	Ln_{NSE} Daily
CAL	+7	+16	0.71	0.68
VAL	−12	0	0.66	0.86
Overall	−3	+7	0.68	0.78

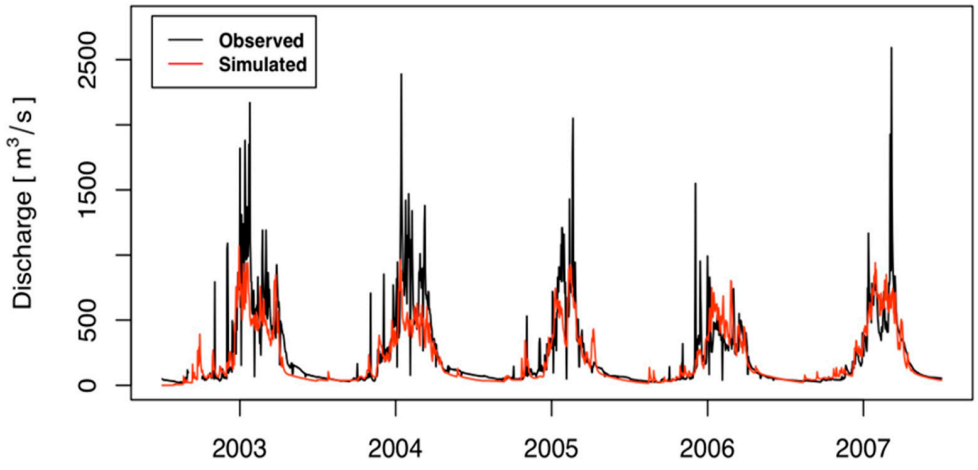

(**a**)

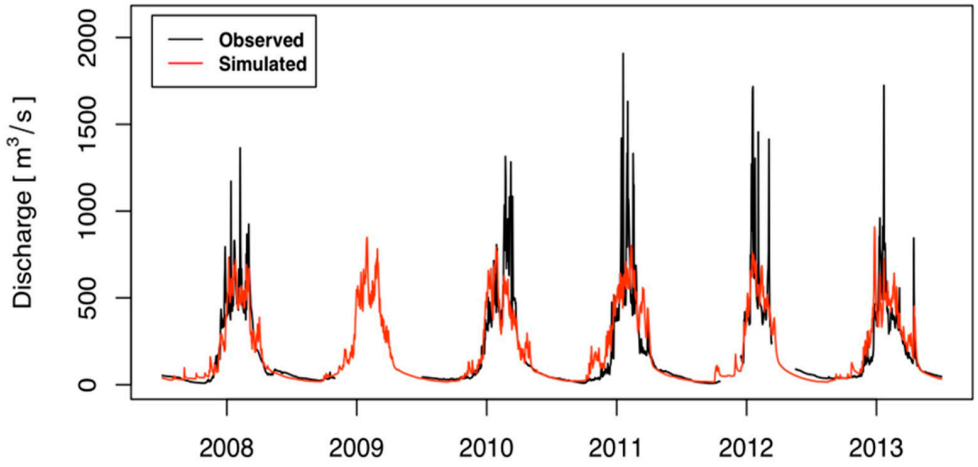

(**b**)

Figure 4. Observed and simulated daily flow using *Poli-Hydro* at Rabuwa Bazar. (**a**) *CAL*. (**b**) *VAL*.

However, given the complex hydrology of the catchment, and the large difficulties in proper flow estimation thereby, as widely reported in the literature (e.g., [74]), the model provides an acceptable flow depiction for the purpose here, i.e., for hydropower assessment.

5.2. Poli-ROR

Since heuristic optimization is sensitive to three main parameters n_r, L_{max}, and α, we carried out a sensitivity analysis, SA. We used both optimization approaches, *Min-LCOE*, *M1* and *Max-Connection*, *M2*. In Figure 5 we report the results of the SA, focusing upon the number of connected villages. Particularly, it is shown therein the SA of n_r and L_{max} (with $\alpha = 0.5$). To assess the performances of the model with different input parameters, we varied the number of initial clusters n_r within 10–100,

with steps of 10 units, while for L_{max} values of 1500, 2000 and 2500 m were selected. On the x axis, it is reported the final number of clusters n_r (which may differ slightly from the initial value, because the algorithm automatically removes mini-grids able to connect few villages). Figure 5a,b display on the y axis the share of connected villages globally (*M1*, *M2*), against n_r. L_{max} is relevant, because the larger L_{max}, the larger the share. Increasing n_r above a certain value (ca. n_r = 20) does not largely change the share of villages connected.

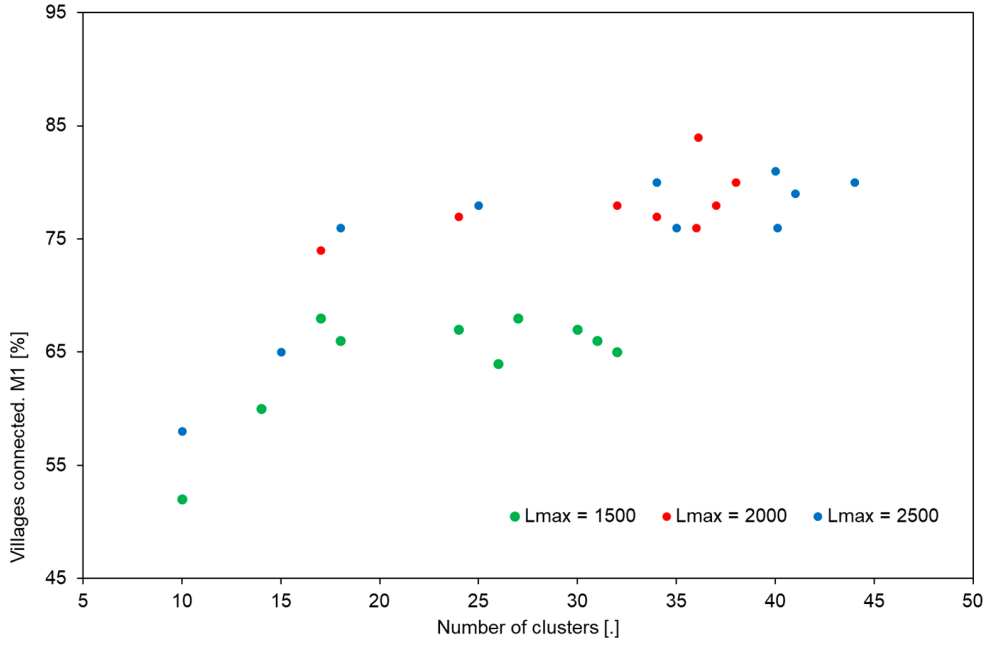

(**a**)

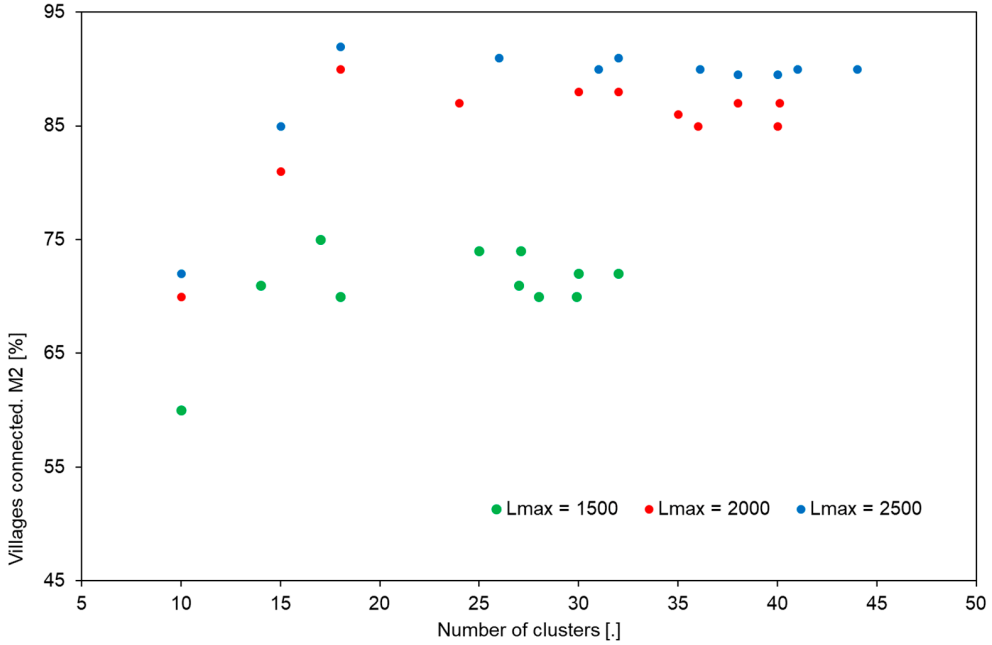

(**b**)

Figure 5. Sensitivity analysis, SA of *Poli-ROR* against the number of clusters/plants n_r, and the maximum length of the transmission line between two villages *Lmax*. (**a**) Connected villages, *Min-LCOE* approach *M1*. (**b**) Connected villages, *Max-Connection* approach *M2*.

A similar analysis (not shown for shortness) of *LCOE*, demonstrated that an increase in n_r tends to increase the average cost of electricity, with values from 0.064 to 0.084 € kWh^{-1}. This may be because more mini-grids, and thus smaller plants in terms of nominal power, do not profit from scale effects. Apparently, no large influence of L_{max} is seen.

We then pursued an SA against the parameter α (0–1), quantifying the relative importance of *RI*, and *DI* for assessment of the grid generation score *GGS* in Equation (8), using different values of L_{max}, and of number of initial clusters n_r. Similar results were however obtained for different values of L_{max}, and n_r. The results are not shown here for shortness (see [86]), but shortly commented. Both with *M1*, and *M2*, an increase in α decreases the average *LCOE*, and larger changes are observed within α = 0–0.5. This seems in accordance with the meaning of the resource indicator *RI*, which evaluates the economical convenience of producing energy from a given hydro-power plant. Accordingly, a higher weight applied to such indicator results into a minor cost of the final configuration. Concerning the share of served villages, giving more importance to the demand concentration upon a plant *DI* (i.e., decreasing α in Equation (8) should result into a greater number of villages served. However, no large variation is observed when using *M1* (*Min-LCOE*) method (with the exception of α = 0), and even an opposite trend is seen using *M2* (*Max-Connection*), with saturation to ca. 90% of villages served for α = 0.5 or so. As a possible explanation one may state that giving more importance to *DI* results into less, or even no importance of the hydro-power plant capacity. Therefore, it may happen that, even though a plant is surrounded by high demand, it would not have the sufficient capacity to satisfy such demand fully. This is especially true for the *M2* method, which tends to create more extended mini-grids. According to the results of the SA, one can conclude that *Poli-ROR* algorithm is stable, and leads to better grid design for $0.5 < \alpha < 1$. For eolic, and photovoltaic based mini-grids, Ranaboldo et al. [79] obtained a somewhat different set of values ($0 < \alpha < 0.5$). However, this may be because hydro-power is more site-dependent, with respect to the other two sources. We thus decided to select a value of α = 0.5, fit in both ranges.

Since the primary objective of the study is to serve the highest possible share of the population, and further doing so at the least cost, the best solution here seems the one obtained using method *M2* (L_{max} = 2500, n_r = 19, α = 0.5), leading to 93% of connected villages, with a relatively low *LCOE* of 0.068 € kWh^{-1}, comparable to the cost of purchasing electricity from the Nepalese electrical grid, which varies from 0.042–0.07 € kWh^{-1}, depending on the hour of the day. Moreover, even though some failure occurs (i.e., at times, energy demand cannot be met fully), even in the worst-case scenario, ca. 87% of the daily energy demand is satisfied. A summary of the characteristics of the so designed mini-grid is reported in Table 6. In Figure 6, the mini-grid (designed plants) is sketched, with indication of the failure days per year n_f.

Table 6. *Poli-ROR*. Optimal solution. Characteristics of the best mini-grid (see Figure 6) designed (Methods *M2*, L_{max} = 2500, n_r = 19, α = 0.5). *ID* is identification code for the plant. ΔH_{gross} is vertical jump (before hydraulic losses), Q_{max} is maximum nominal flow, P_{nom} is nominal power, $E_{supplied}$ is daily mean energy produced, S_d is drainage area of the basin, n_f is number of days with failure, $e_{def\%}$, maximum percentage daily deficit.

ID	ΔH_{gross} (m)	Q_{max} (m^3 s^{-1})	P_{nom} (kW)	$E_{supplied}$ (MWh day^{-1})	S_d (km^2)	Villages	*LCOE* (€ kWh^{-1})	n_f (day)	$e_{def\%}$ (%)
1	69	1.79	1211	25.3	480	88	0.06	0	0
2	83	1.12	911	17.6	350	65	0.07	24	13
3	114	0.46	514	10.7	520	34	0.06	0	0
4	244	0.31	750	15.6	500	53	0.05	0	0
5	93	0.94	858	17.9	610	51	0.06	0	0
6	45	2.39	1054	19.0	3580	59	0.07	0	0
7	354	0.16	544	11.3	1700	32	0.05	0	0
8	117	0.72	823	17.2	1100	58	0.06	0	0

Table 6. *Cont.*

ID	ΔH_{gross} (m)	Q_{max} (m^3 s^{-1})	P_{nom} (kW)	$E_{supplied}$ (MWh day^{-1})	S_d (km^2)	Villages	*LCOE* (€ kWh^{-1})	n_f (day)	$e_{def\%}$ (%)
9	80	0.18	140	2.9	1200	30	0.11	0	0
10	70	0.55	380	7.9	1250	33	0.07	0	0
11	120	0.95	1118	23.3	2100	74	0.05	0	0
12	180	0.07	125	2.6	750	45	0.14	0	0
13	169	0.77	1271	25.0	350	75	0.06	21	11
14	89	1.00	870	18.1	320	61	0.06	0	0
15	70	0.98	671	13.1	210	41	0.08	21	12
16	92	0.73	656	13.7	230	38	0.07	0	0
17	106	0.57	594	12.2	110	52	0.07	11	6
18	281	0.33	896	18.5	720	49	0.05	8	4
19	145	0.57	810	15.9	140	38	0.05	21	10

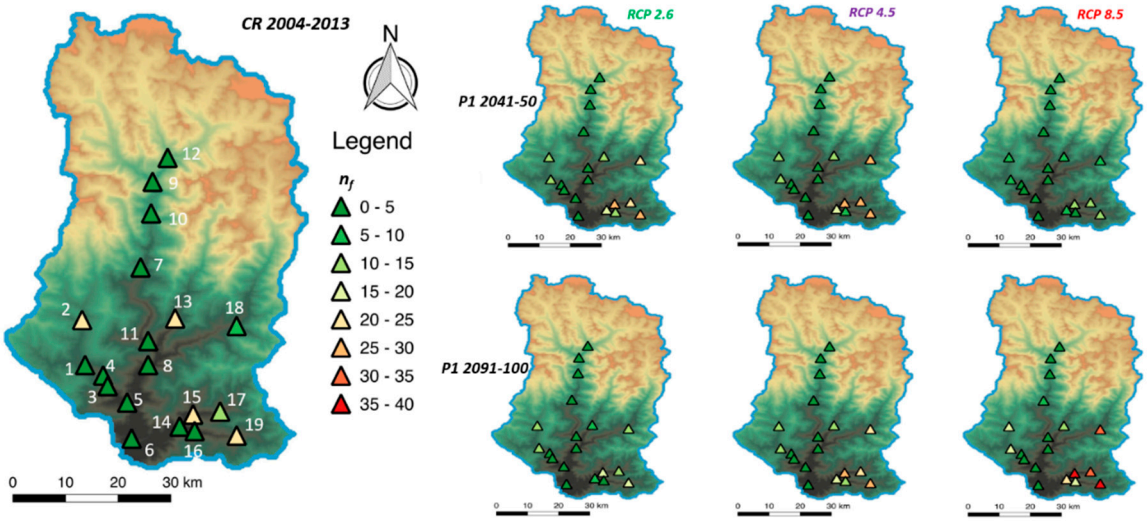

Figure 6. Designed grid. Average number of failure days n_f. Control run *CR*, and projected future decades *P1*, *P2* (averages between the three models under the three RCPs, 2.6, 4.5, 8.5).

5.3. Future Flows, and Hydropower Potential

We focus here upon two specific time-windows, or periods. Period 1 *P1* is at mid-century (2041–2050), while period 2 *P2* is at the end of century (2091–2100). In Figure 7 below we report mean annual variations (percentage) of precipitation $\Delta P_{\%}$, and stream flows $\Delta Q_{\%}$, for *P1*, and *P2*, against the control run period *CR* (2004–2013), for different RCPs, and GCMs, plus the mean value for each RCP. Precipitation variations would be mostly positive during *P1*, *P2*. On average precipitation would increase by +7.5% in *P1*, and +8.5 during *P2*, with large variability; however, with visible projected decrease (−5.98%) only under RCP8.5 of ECHAM6 at half a century [11,66,71].

Stream flows are also mostly increasing, but in some scenarios decrease may be seen (especially for RCP2.6 during P2). On average, between GCM models one has in *P1* $\Delta Q_{\%}$ = +4.3%, +5.9%, and +2.5% under RCP2.6, 4.5, and 8.5, respectively. In *P2*, one has on average $\Delta Q_{\%}$ = −1.2%, −0.6%, and +7.9% under RCP2.6, 4.5, and 8.5, respectively. Under the temperature increase as projected in RCPs 4.5, and RCP 8.5 (RCP2.6, +0.50 °C, +0.41, RCP4.5, +0.85 °C, +1.72 °C, RCP8.5, +1.72 °C, +4.31 °C, at *P1*, and *P2*, on average), ice volumes in the catchment will be reduced, so possibly reducing stream flows in the highest areas [71]. Monthly, slight increase would be seen during September to April (dry season, not shown, see [86]), with slight decrease during monsoon, due to both decreased ice volume, and precipitation. In Figure 8 below we report flow duration curves at Rabuwa bazar, during CR, and averaged (between three GCMs) for each RCP during *P1*, and *P2*.

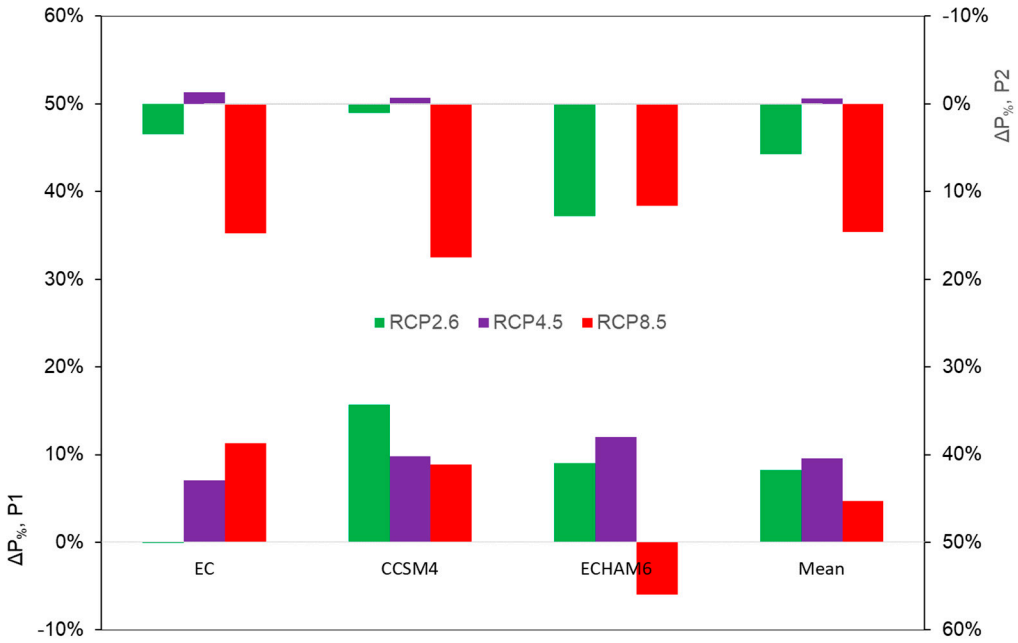

(**a**)

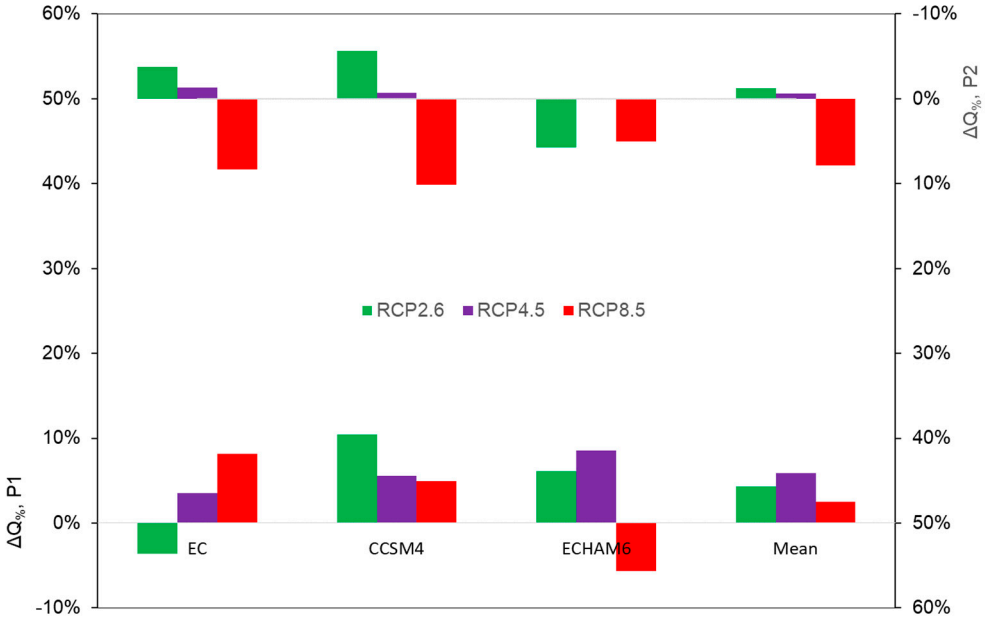

(**b**)

Figure 7. Rabuwa Bazar. Mean annual variations (in percentage) for the decades *P1*, 2041–2050 (left *y* axis), and *P2* 2091–2100 (right *y* axis, values upside down), against *CR* period (2004–2013). (**a**) Precipitation. (**b**) Streamflows.

From Figure 8 above, at half century *P1*, flow duration would not change largely from now. Conversely, at the end of century *P2*, low flows (i.e., for duration 180+ days) would increase, at least at the basin outlet in Rabuwa, which would suggest increase of hydropower potential (i.e., for the highest discharges, or longer periods of flow above turbine capacity). However, the potential for

change of production depends upon complex interaction of stream flow, and turbine capacity for each hydropower station.

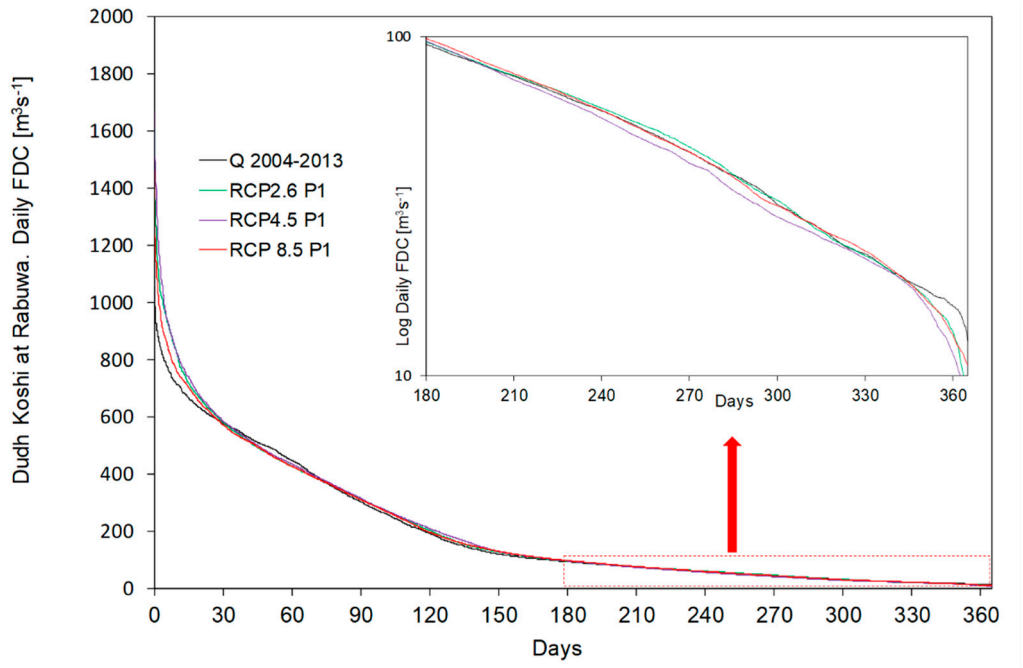

(**a**)

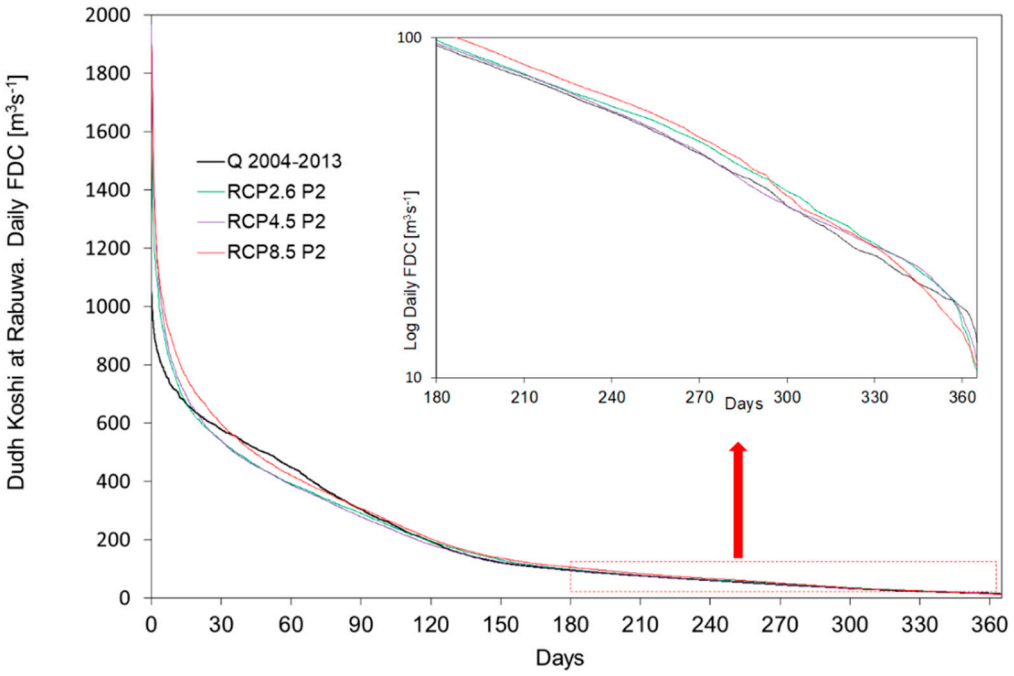

(**b**)

Figure 8. Rabuwa bazar. Flow duration curves. CR, and average (three GCMs) for each RCP. (**a**) *P1*. (**b**) *P2*. Logarithmic values are used in the window to highlight low flows for longest durations.

To test the performances of the designed grid under our potential future hydrological scenarios, we used the projected flow duration curves during *P1*, and *P2* as inputs to *Poli-ROR*, to calculate the corresponding hydropower potential. As reported, we assessed the average number of failure days

per year n_f, and the maximum daily energy deficit per year $e_{def\%}$. Figure 9 below reports graphically the average (between the three GCMs) projected number of n_f, and $e_{def\%}$ for *P1*, and *P2* under our three RCPs for the different plants, in numerical order (see location of the plants in Figure 6, Section 5.2).

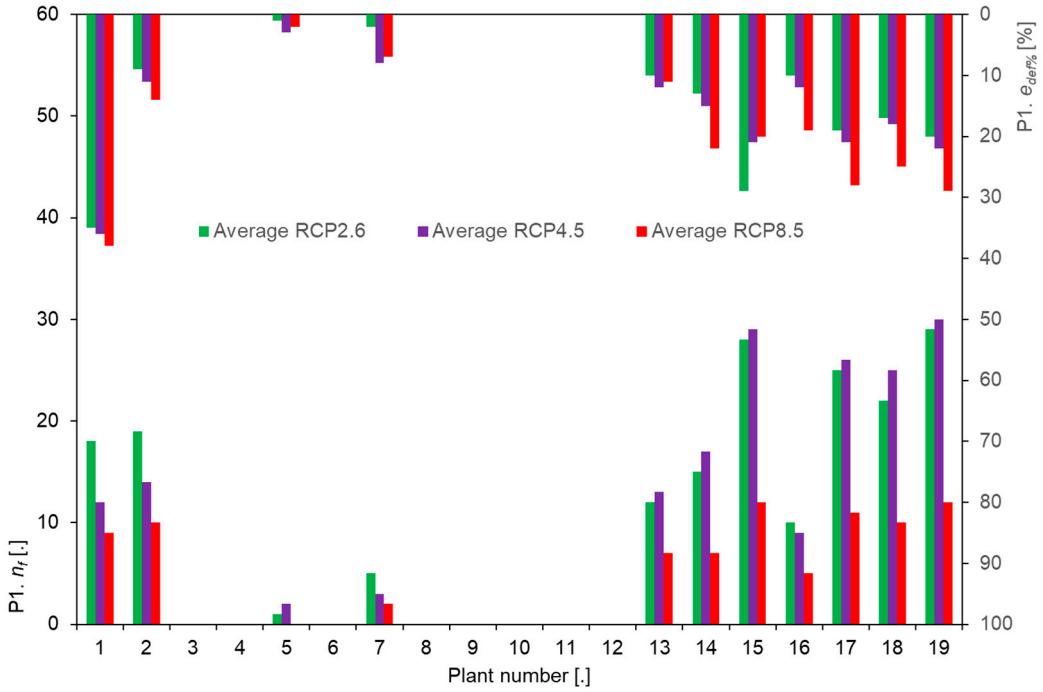

(**a**)

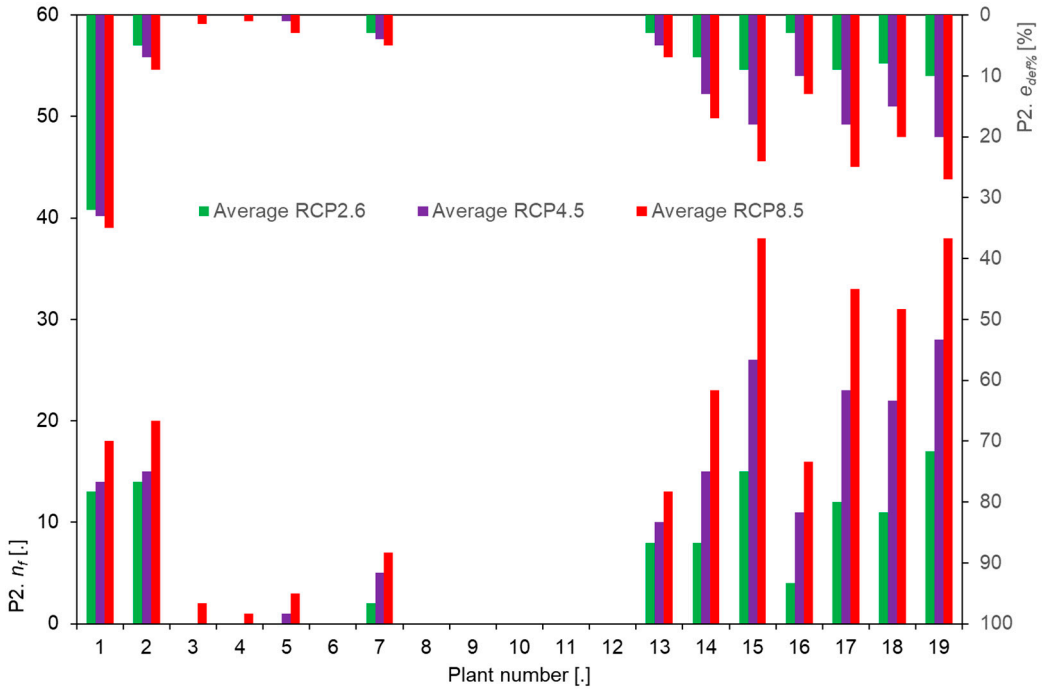

(**b**)

Figure 9. Designed grid. Average (three GCMs) projected number of failure days n_f (left *y* axis) and maximum percentage energy deficit $e_{def\%}$ (right *y* axis, values upside down) for each RCP. (**a**) *P1*. (**b**) *P2*.

From Table 6, Figure 6 (Section 5.2), and Figure 9 above, one finds that *ROR* plants that drain the largest catchments, and in general plants along the main stem of the river, are less (little) affected, given that their nominal discharge (Q_{max}) is small (marginal) with respect to normal flows. In the smallest (highest) catchments, during *P1*, and *P2* $e_{def\%}$ increases from RCP 2.6 to RCP 8.5, reaching 20% or more (in the S-E area in Figure 6).

During *P1* under RCP, 8.5 n_f is the smallest, while during *P2* it increases with the RCP. This is possibly due to a large ice melt contribution during *P1* under the warmest RCP8.5, which initially provides additional flows at thaw. However, during *P2* ice would be largely depleted under RCP8.5, and n_f increases accordingly. Compared to *CR*, a great number of the designed plants showed a decline of performances. In the worst case, the inhabitants will not be covered for ca. 40 days (plants 15, 19) per year (vs. 24 under historical conditions, plant 2), and will further have a least energy production of ca. 60% (plant 1) of their demand (87% under historical conditions, plant 2).

6. Discussion

6.1. Improvement in Grid Design Using Poli-ROR

The heuristic construction procedure we used here as a base was developed for wind, and solar systems [79], and did not include the clustering step, which we introduced originally. This step was necessary because of the inherently different characteristics of hydropower networks. The original methodology, when applied to the hydropower problem, provided physically unfeasible networks. For instance, the designed grids may overlap on one another, with crossing of cables, and pipes. Water resources in a catchment is distributed along a (river) network, and not homogeneously spread like wind or radiation, and accordingly there is only one set of possible generation (source) points, belonging to the river. Moreover, hydropower plants generally require a larger nominal power, to produce energy with competitive price. Therefore, they are usually not convenient either for stand-alone systems, or for very small grids, and due to their branching nature, extended distribution networks are more prone to overlapping. To overcome this issue, we sought to partition the catchment in clusters as reported. Each cluster has a set of villages, inlet and outlet points, starting from which one mini-grid is designed, avoiding overlapping, and other unacceptable features.

Here we provide a comparison between the two methods, to give an insight of the gain from the clustering step. In Figure 10, we report the designed network obtained using the original method by Ranaboldo et al. [79], and the *Poli-ROR* algorithm (method *M2*). We used here L_{max} = 2500, and α = 0.5, and a layout with an equal number of mini-grids, n_r = 24, for fair comparison. Visually, the Ranaboldo et al. [79] model constructs more branched grids with respect to *Poli-ROR*. This leads to a major drawback, that transmissions lines belonging to one grid tend to intersect with those from other grids, as reported. In facts, at each step the original method looks out for the local optimum of each plant, and shapes the best mini-grid configuration (in terms of *LCOE*), considering only the demand points that have not been connected yet. As a result, the last mini-grids designed will try to connect very sparse demand points, with a high chance of intersecting already existing connections.

An example is seen in Figure 10a, where the original algorithm provides in the Central-Western part of the catchment two grids, namely grid 1 (dark red dots), and grid 17 (light green dots), very sparse, and displaying long connection patterns. Conversely, in Figure 10b, our algorithm provides three different grids (1, dark red 5, light red, 10, yellow) in the same area, that are much smaller and better clustered, thereby decreasing the mean connection length, related cost, and chance of intersection.

Similarly, in the South-Eastern part of the basin in Figure 10a, one has less organized, overlapping grids (especially 9, orange, and 22, light blue), whereas in Figure 10b, much better clustered grids are provided [24,33,59,87].

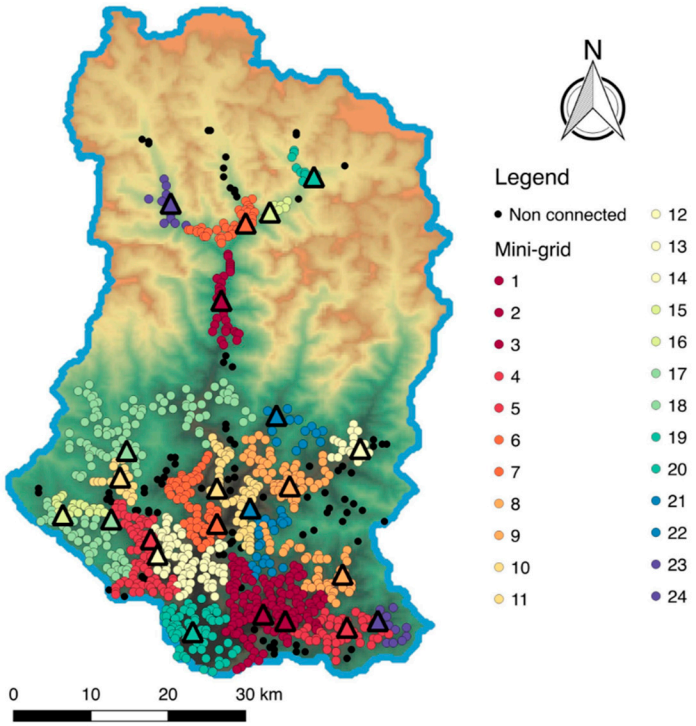

(**a**)

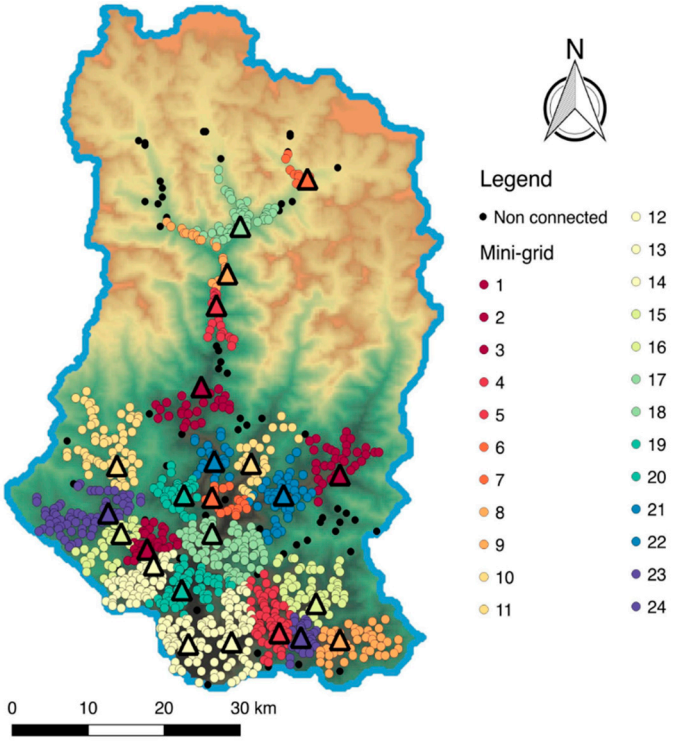

(**b**)

Figure 10. Visual layout of the designed mini-grids using the original clustering method by Ranaboldo et al. [80], and *Poli-ROR*. Each color represents a mini-grid with the corresponding demand points (villages), and the designed hydro-power plants (triangles). A fixed number of clusters $n_r = 24$ as from the method by Ranaboldo et al. [80] is used for reference. (**a**) Ranaboldo et al. [80]. (**b**) *Poli-ROR*.

Another drawback of the method is that there is no control over the desired number of production points. Contrarily, in *Poli-ROR* the areas of influence for each plants are predefined, so that each demand point is tentatively connected to the closest plant. In addition, a better control on the desired number of hydro-power plants can be exerted, specifying the initial number of cluster n_r. Differences also occur in terms of energy cost. The original algorithm finds a configuration with an average *LCOE* = 0.091 € kWh^{-1}, +34% than the one determined by *Poli-ROR*, *LCOE* = 0.068 € kWh^{-1}. Since the expansion process of the original algorithm aims at reaching the minimum local cost of each mini-grid, at each step some villages are obviously excluded. Most of the time, such villages are the ones located the furthest away from water. As a consequence, trying to connect them independently or with small mini-grids will result in a high per capita cost. Based on some sensitivity analysis upon L_{max}, the only variable parameter in the original method (not shown, see Manara [86]), we found that the original model is always among the subsets with the worst economical performances, with an average *LCOE* considerably higher, and a share of connected villages nearby 90% or so, slightly lower than the best solution from *Poli-ROR* (93%). As such, *Poli-ROR* provides an improved approach to network design, namely one with a (much) lower cost as from *LCOE*, and a more feasible spatial pattern.

6.2. Potentially Modified Hydropower Potential under Climate Change

Climate change modifies the hydrological cycle, which clearly affects water resources availability. Among others, Soncini et al. [71] studied future flows in the upper part (closed at Periche) of the Dudh Koshi basin. In that study, the authors found that for such high altitude catchment, stream flows would increase in monsoon season, but would decrease yearly (−4% vs. *CR* on average) during 2045–2054. At the end of the century, a large reduction would occur in all seasons, i.e., −26% on average during 2090–2099.

Here, we found mostly increased streamflow overall, which suggests that future precipitation (and rainfall during monsoon) will be the most defining factor of hydropower potential.

Among others, Gautam et al. [26] suggested that hydropower plants in the Himalayas will suffer increasingly from climate change henceforth, especially those relying heavily upon the buffering of high altitude snow/ice reservoirs. Pathak [88] put forward that the increasing trend of glacial retreat, the variability of temperature, and precipitation may impact water resources and hydropower development in Nepal. Decreased runoff may affect hydropower development, but there is large uncertainty about future spatial variability of climate drivers. Here we found that the highest plants taking water from the smallest catchments would be more sensitive. However, the definition of the vulnerability depends upon complex topography, and climate, and requires accurate local hydrological modeling. Shrestha et al. [71] studied modified discharges in the Kulekhani watershed due to climate change, and power generation from the regulated Kulekhani reservoir. They considered future climate conditions from the A2 and B2 scenarios of the HadCM3 GCM for three periods (2010–2039, 2040–2069 and 2070–2099). They projected decreased yearly precipitation in all periods, with a decrease in precipitation/stream flows during the wet months (May–September), and increase during the dry months (October to April). Assuming hydropower plant operations for 7 h per day during CR period (1982–2009), average power production was projected to decrease by −30% for A2 and B2 scenarios. Here, under potentially constant, or even increased stream flows in response to increased precipitation, the hydropower network may perform worse in some nodes. Clearly, in our case, given the lack of storage in *ROR* schemes, potentially buffering for water shortage period [89], the grid may suffer from periods of low flows, especially during the dry season. Notice that one may design the mini grid by feeding *Poli-ROR* with projected future stream flow series, maybe under a worst case scenario approach. This exercise was not pursued, as it is beyond the scope of the present work, but it may be of interest for future developments.

Among others, Hussain et al. [27] provided further ground for investigating the impact of climate change upon hydropower development in the Himalayas. They suggested that climate change induced extreme events are also major challenges to hydropower infrastructures (e.g., for rapidly enlarging

glacial lakes GLs, [87]). Such facets require further investigation, and coupling hydropower risk analysis with glacio-hydrological models may help in this effort.

6.3. Limitations, and Outlooks

Some limitations may have hampered the current study, and development of *Poli-Hydro*, and *Poli-ROR* models. The low spatial density of meteorological stations and the relatively high percentage of missing data in the series made the hydrological modelling particularly challenging, especially for precipitation, which is knowingly characterized by an extremely high spatial variability in the complex Himalayan topography [58]. Data requirements for hydrological modeling, and portability of *Poli-Hydro* model are discussed elsewhere (e.g., [49]), and hydro-meteorological information is necessary. It should be noted that one could indeed use observed stream flows—although these are seldom measured over a dense network of stations—as required for spatially distributed assessment. However, if one was interested in hydrological projections pending future climate scenarios, hydrological modeling would be warranted. In cryospheric driven catchments such as those explored here, modeling of the snow/ice component seems necessary, at least in the high altitudes, and field data may be necessary. Here, we could exploit the findings of former studies.

Some limitations to application of the *Poli-ROR* algorithm were given by sparse information of population distribution, and their present and forecast energy demand. The grids were further designed under the simplistic hypothesis of being completely powered by hydropower energy, which made it necessary to limit the maximum nominal flow at each plant, to provide dependable energy production as far as possible. Despite such assumptions, and thanks to the abundance of water in the region, it was possible to largely fulfil energy demand. Whenever applying the method to other contexts, integration with other energy sources must be explored.

Some future developments may therefore be sketched. First, one would need to survey the actual spatial distribution of the population and their energy consumption patterns, including their variation in space and time, also to evaluate need of batteries to balance daily fluctuations. Moreover, since the use of electrical storage systems is not a viable option even for few days, one needs to explore the feasibility of (small) water storage, and/or backup generators. One could modify *Poli-ROR* to support planning of hybrid mini-grids, based on a mix of renewable energy sources (i.e., solar, wind). Moreover, it would be of interest to test the *Poli-ROR* algorithm to other study areas, to evaluate its performance and robustness.

Mini-hydro is a cost-competitive solution for rural electrification when adequately planned. Funding support programs in this direction could dramatically improve the living quality of the inhabitants, and as well decrease the pressure on the surrounding environment, still fostering tourism in this largely visited region. Even at a national level, exploiting the richness of the water resource could be an optimal strategy to mitigate pollution, and move to renewable energy sources. Models explicitly coupling catchment scale/regional hydrological modeling and hydropower potential analysis, including the potential effects of future climate change as we did here, may be of help in this effort.

Our study presents a tool to preliminarily assess hydropower potential, under a basin scale assessment. Clearly, details of the construction of specific *ROR* plants would need to be discussed based upon specific local focus. The design and construction of *ROR* plants indeed pose some critical points.

The presence of *ROR* schemes, and generally of hydropower plants, may impact river flow. Here, no reservoir is designed, so no regulation will occur. Moreover, we explicitly included a consideration of environmental flow release downstream of each plant in our analysis, to maintain the acceptable hydro-morphic quality of the river. However, in the design and construction phase of *ROR* plants, specific attention would be devoted to environmental conditions in the stream.

Furthermore, the design of each *ROR* power plant will have to include proper sediment load management (trapping structures, trapping efficiency, periodic removal via flushing, scouring, or trucking), which will require site-specific assessment. Recent studies provide large scale estimates of sediment load within the mountain catchments of Nepal, and within Koshi river, including Dudh

Koshi here. Among others, Sangroula [15] reported sediment sampling at Chatara station of Koshi river, showing an average amount of annual sediment yield in the order of 2800 ton km^{-2} $year^{-1}$. Accordingly, sediment management in the area is critical.

The construction and operation of hydropower plants in topographically and societally complex areas of the Himalayas is a complex topic, with large socio-economic and political implications (e.g., [90,91]).

Overall, locally produced hydropower may give benefits to local people, possibly helping touristic activity, and reducing the pollution produced through the burning of kerosene, and other fuels for heating/cooking, as done nowadays.

A main risk associated with hydropower development in Nepal, and generally in the Himalayas, clearly relates to collapse of (large) dams and subsequent flood propagation in the wake of a geological (e.g., landslide), hydro-meteorological (e.g., flood), glacial (e.g., glacial lake outburst floods, GLOFs), or seismic (earthquake) event [90].

Given that *ROR* plants do not require large, potentially dangerous water storage, the risk for the downstream population may be decreased in this sense.

Potential topographic, and geomorphological changes in the catchment were not addressed here. The Koshi catchment overall is quite large. So, unless for very small headwater catchments, one can expect that local changes, possibly related to rapid mass movements such as landslides or debris flows, or transitions from glacial to not glacial landscapes, would not change largely hydrology.

Nor have we accounted here for seismic activity—however knowingly intense. Seismic activity, in our understanding, may affect *ROR* schemes in two possible ways; namely, (i) by damaging the network, and (ii) by modifying topography (i.e., causing changes in the landscape by faulting, and triggering landslides, etc.), with fallout upon hydrology, and energy production.

Accordingly, once the *ROR* network is designed, it should be then built according to anti-seismic rules and regulations, independently of the climate.

Notice also that a distributed *ROR* network may be more resilient in the face of natural disasters, because it is unlikely that all plants would break down at the same time.

However, the topic of network reliability against natural hazards does not fall strictly within the purview of hydrological sciences, and it clearly needs be tackled in further studies.

7. Conclusions

Nepal has large potential for hydropower production, to offset large use of fossil fuels, and air pollution thereby. Hydropower planning and implementation, both as (i) micro-hydro with *ROR* systems, and (ii) large hydropower regulation, is very necessary, especially in the face of the changing climate and increasing energy demand henceforth. In this study, we coupled a state of the art hydrological model *Poli-Hydro*, suitable for mimicking the complex hydrology of high altitude catchments, with a heuristic algorithm *Poli-ROR*¸ to pursue the exercise of designing a mini hydro-power grid for the topographically complex Dudh Koshi catchment at the toe of mount Everest. *Poli-ROR* is based upon some demand-production indicators proposed in the present literature, and on the spatial distribution of the settlements to be served. *Poli-ROR* was compared against another recent design algorithm for energy grid design, providing evidence of some improvement. The resilience of the electrification scheme to potential future changes of climate/hydrology was also verified. We showed that mini-hydro here may be a suitable technology, able to satisfy local energy demand for 90% + of the population, with a cost comparable to that on the national grid. However, due to lack of storage, some plants may not be able to fully supply energy requirements for few days a year. This mismatch may be exacerbated, especially for those scenarios with the highest values of radiative forcing, and bring large cryospheric depletion at the highest altitudes. The method developed here profits from a knowledge of the hydrological processes within the case study catchment, and therefore requires basic hydrological information and modelling. However, at the cost of reasonable hydrological data gathering and subsequent modelling, the *Poli-ROR* algorithm is a powerful tool—usable for

supporting the long-term design of *ROR* schemes, and generally for planning at a regional level. *Poli-ROR* surely provides a link between general, basin scale hydropower potential assessment, and subsequent site-specific analysis, that can be scaled and applied to other areas and topographically complex catchments. The presence of *ROR* schemes in the area may provide tremendous benefit to the population locally, by decreasing pollution, increasing the available energy, and fostering sustainable tourism; therefore, our preliminary findings may be of great use in this sense for scientists, water managers, policy makers.

Hydropower development in this area clearly does not only encompass technical issues, but it entails a large array of socio-economic and political implications. Within this complex framework, our approach may provide a technical help to hydropower planning.

Author Contributions: D.B., field campaigns in Nepal, data gathering, project coordination, hydrological model set up, paper writing. M.M., *Poli-Hydro* model set up, *ROR* scheme optimization algorithm, climate-hydrological scenarios. R.M., energy grid assessment, strategic choices for *ROR* power plants, hydropower calculation. All authors have read and agreed to the published version of the manuscript.

Funding: This research received no external funding.

Acknowledgments: We hereby acknowledge the Department of Hydro Meteorology (DHM) of Nepal, for providing weather, and hydro data from their stations. The EVK2CNR Pyramid staff are kindly acknowledged for sharing data, and information. We acknowledge the World Climate Research Program's Working Group on Coupled Modelling, which is responsible for CMIP5, and we thank the climate modeling for producing and making available their model outputs. Eng. Andrea Soncini, PhD, is kindly acknowledged for help with use of *Poli-Hydro* in fulfilment of Eng. Manara Master Thesis. The authors acknowledge support from personnel of *Climate-Lab* (https://www.climatelab.polimi.it/en/), the Interdepartmental Laboratory on Climate Change at Politecnico di Milano, for climate change projections, downscaling, hydrological modelling.

Conflicts of Interest: The authors declare no conflict of interest.

References

1. United Nations Organization. The 2030 Agenda for Sustainable Development. Available online: https://www.un.org/ga/search/view_doc.asp?symbol=A/RES/70/1&Lang=E (accessed on 18 September 2020).
2. International Energy Agency IEA. *Special Report: Energy Access Outlook*; IEA: Paris, France, 2017.
3. Nerini, F.F.; Broad, O.; Mentis, D.; Welsch, M.; Bazilian, M.; Howells, M. A cost comparison of technology approaches for improving access to electricity services. *Energy* **2016**, *95*, 255–265. [CrossRef]
4. IRENA. Innovation Outlook Renewable Mini-grids. 2016. Available online: https://www.irena.org/publications/2016/Sep/Innovation-Outlook-Renewable-mini-grids (accessed on 18 September 2020).
5. Karki, R.; Gurung, A. An Overview of Climate Change And Its Impact on Agriculture: A Review From Least Developing Country, Nepal. *Int. J. Ecosyst.* **2012**, *2*, 19–24. [CrossRef]
6. OXFAM. *Even the Himalayas Have Stopped Smiling: Climate Change, Poverty and Adaptation in Nepal*; Oxfam International, Country Programme Office: Lalitpur, Nepal, 2009.
7. Immerzeel, W.W.; van Beek, L.P.H.; Bierkens, M.F.P. Climate Change Will Affect the Asian Water Towers. *Science* **2010**, *328*, 1382–1385. [CrossRef] [PubMed]
8. Immerzeel, W.; Petersen, L.; Ragettli, S.; Pellicciotti, F. The importance of observed gradients of air temperature and precipitation for modeling runoff from a glacierized watershed in the Nepalese Himalayas. *Water Resour. Res.* **2014**, *50*, 2212–2226. [CrossRef]
9. Bocchiola, D. Agriculture and food security under climate change in Nepal. *Adv. Plants Agric. Res.* **2017**, 6. [CrossRef]
10. Konar, M.; Dalin, C.; Suweis, S.; Hanasaki, N.; Rinaldo, A.; Rodriguez-Iturbe, I. Water for food: The global virtual water trade network. *Water Resour. Res.* **2011**, *47*, W05520. [CrossRef]
11. Palazzoli, I.; Maskey, S.; Uhlenbrook, S.; Nana, E.; Bocchiola, D. Impact of prospective climate change upon water resources and crop yield in the Indrawati basin, Nepal. *Agric. Syst.* **2015**, *133C*, 143–157. [CrossRef]
12. Chalise, S.R.; Kansakar, S.R.; Rees, G.; Croker, K.; Zaidman, M. Management of water resources and low flow estimation for the Himalayan basins of Nepal. *J. Hydrol.* **2003**, *282*, 25–35. [CrossRef]
13. Rees, H.G.; Holmes, M.G.R.; Fry, M.J.; Young, A.R.; Pitson, D.G.; Kansakar, S.R. An integrated water resource management tool for the Himalayan region. *Environ. Modell. Softw.* **2006**, *21*, 1001–1012. [CrossRef]

14. Mainali, B.; Silveira, S. Financing off-grid rural electrification: Country case. *Nepal Energy* **2011**, *36*, 2194–2201. [CrossRef]
15. Sangroula, D.P. Hydropower development and its sustainability with respect to sedimentation in Nepal. *J. Inst. Eng.* **2009**, *7*, 1–9. [CrossRef]
16. Nepal, R. Roles and potentials of renewable energy in less-developed economies: The case of Nepal. *Renew.·Sustain. Energy Rev.* **2012**, *16*, 2200–2206. [CrossRef]
17. Sanchez, T.; Dennis, R.; Pullen, K.R. Cooking and lighting habits in rural Nepal and Uganda. *J. Power Energy* **2013**, *227*, 727–739. [CrossRef]
18. Houghton, J.T.; Ding, Y.; Griggs, D.J.; Noguer, M.; van der Linden, P.J.; Dai, X.; Maskell, K.; Johnson, C.A. Contribution of working group I to the third assessment report of the intergovernmental panel on climate change. In *Climate Change 2001: The Scientific Basis*; Cambridge University Press: Cambridge, UK, 2001.
19. Parajuli, I.; Lee, H.; Shrestha, K.R. Indoor air quality and ventilation assessment of rural mountainous households of Nepal. *Int. J. Sustain. Built Environ.* **2016**, *5*, 301–311. [CrossRef]
20. Pokharel, S. Kyoto protocol and Nepal's energy sector. *Energy Policy* **2007**, *35*, 2514–2525. [CrossRef]
21. Sharma, C.K. Overview of Nepal's energy sources and environment. *Atmospheric Environ.* **1996**, *30*, 2717–2720. [CrossRef]
22. Soncini, A.; Bocchiola, D.; Confortola, G.; Minora, U.; Vuillermoz, E.; Salerno, F.; Viviano, G.; Shrestha, D.; Senese, A.; Smiraglia, C.; et al. Future hydrological regimes and glacier cover in the Everest region: The case study of the Dudh Koshi basin. *Sci. Total Environ.* **2016**, *565*, 1084–1095. [CrossRef]
23. Thakuri, S.; Salerno, F.; Smiraglia, C.; Bolch, T.; D'Agata, C.; Viviano, G.; Tartari, G. Tracing glacier changes since the 1960s on the south slope of Mt. Everest (central Southern Himalaya) using optical satellite imagery. *Cryosphere* **2014**, *8*, 1297–1315. [CrossRef]
24. Devkota, L.P.; Gyawali, D.R. Impacts of climate change on hydrological regime and water resources management of the Koshi River Basin. *Nepal J. Hydrol. Reg. Stud.* **2015**, *4*, 502–515. [CrossRef]
25. Bocchiola, D.; Soncini, A. Water resources modeling and prospective evaluation in the Indus River under present and prospective climate change. In *Indus River Basin: Water Security and Sustainability*; Khan, S., Adams, T., Eds.; Elsevier: Amsterdam, The Netherlands, 2019; p. 500. ISBN 9780128127827.
26. Gautam, B.R.; Li, F.; Ru, G. Climate Change Risk for Hydropower Schemes in Himalayan Region. *Environ. Sci. Technol.* **2014**, *48*, 7702–7703. [CrossRef]
27. Hussain, A.; Sarangi, G.K.; Pandit, A.; Ishaq, S.; Mamnun, N.; Ahmad, B.; Jamil, M.K. Hydropower development in the Hindu Kush Himalayan region: Issues, policies and opportunities. *Renew. Sustain. Energy Rev.* **2019**, *107*, 446–461. [CrossRef]
28. Mishra, S.K.; Hayse, J.; Veselka, T.; Yan, E.; Kayastha, R.B.; LaGory, K.; McDonald, K.; Steiner, N. An integrated assessment approach for estimating the economic impacts of climate change on River systems: An application to hydropower and fisheries in a Himalayan River, Trishuli. *Environ. Sci. Policy* **2018**, *87*, 102–111. [CrossRef]
29. Agarwal, A.; Babel, M.S.; Maskey, S. Analysis of future precipitation in the Koshi River basin, Nepal. *J. Hydrol.* **2014**. [CrossRef]
30. Awasthi, K.D.; Sitaula, B.K.; Singh, B.R.; Bajacharaya, R.M. Land-use change in two Nepalese watersheds: GIS and geomorphometric analysis. *Land Degrad. Dev.* **2002**, *13*, 495–513. [CrossRef]
31. Chhetri, N.; Chaudhary, P.; Tiwari, P.R.; Yadaw, R.B. Institutional and technological innovation: Understanding agricultural adaptation to climate change in Nepal. *Appl. Geogr.* **2012**, *33*, 142–150. [CrossRef]
32. Eriksson, M.; Xu, J.C.; Shrestha, A.B.; Vaidya, R.A.; Santosh, N.; Sandström, K. *The Changing Himalayas: Impact of Climate Change on Water Resources and Livelihoods in the Greater Himalayas*; ICIMOD: Kathmandu, Nepal, 2009; p. 29. ISBN 978-92-9115-111-0.
33. Gentle, P.; Maraseni, T.N. Climate change, poverty and livelihoods: Adaptation practices by rural mountain communities in Nepal. *Environ. Sci. Pol.* **2012**, *21*, 24–34. [CrossRef]
34. Maskey, S.; Uhlenbrook, S.; Ojha, S. An analysis of snow cover changes in the Himalayan region using MODIS snow products and in-situ temperature data. *Clim. Chang.* **2011**, *108*, 391–400. [CrossRef]
35. Nyaupanea, G.P.; Chhetri, N. Vulnerability to Climate Change of Nature-Based Tourism in the Nepalese Himalayas. *Tour. Geogr.* **2009**, *11*, 95–119. [CrossRef]
36. Rai, M. Climate change and agriculture: A Nepalese case. *J. Agric. Environ.* **2007**, *8*, 92–95. [CrossRef]
37. Shrestha, A.B.; Aryal, R. Climate change in Nepal and its impact on Himalayan glaciers. *Reg. Environ. Chang.* **2011**, *11*, 65–77. [CrossRef]

38. Dulal, H.B.; Brodnig, G.; Thakur, H.K.; Green-Onoriose, C. Do the poor have what they need to adapt to climate change? A case study of Nepal. *Local Environ.* **2010**, *15*, 621–635. [CrossRef]
39. USAID. *Nepal Climate Vulnerability Profile*; USAID: Washington, DC, USA, 2012.
40. WECS. *Energy Sector Synopsis Report*; WECS: Kathmandu, Nepal, 2016.
41. Jha, R. Total Run-of-River type Hydropower Potential of Nepal. *Hydro-Nepal* **2010**, *7*, 8–13. [CrossRef]
42. Gianinetto, M.; Polinelli, F.N.; Frassy, F.; Aiello, M.; Rota Nodari, F.; Soncini, A.; Bocchiola, D. Analysis of changes in crop farming in the Dudh Koshi (Nepal) driven by climate changes. In Proceedings of the Earth Resources and Environmental Remote Sensing/GIS Applications, Warsaw, Poland, 5 October 2014. [CrossRef]
43. Bocchiola, D.; Brunetti, L.; Soncini, A.; Polinelli, F.; Gianinetto, M. Impact of climate change on agricultural productivity and food security in the Himalayas: A case study in Nepal. *Agric. Syst.* **2019**, *171*, 113–125. [CrossRef]
44. FAO. *Food and Nutrition Security in Nepal: A Status Report—Ministry of Agricultural Development and Central Bureau of Statistics for the Nepal Component of the FSO Project*; FAO: Rome, Italy, 2016. Available online: http://admin.indiaenvironmentportal.org.in/files/file/Food%20and%20Nutrition%20Security%20in%20Nepal.pdf (accessed on 18 September 2020).
45. Vuillermoz, E.; Cristofanelli, P. Atmospheric Brown Clouds in the Himalayas: First two years of continuous observations at the Nepal Climate Observatory-Pyramid (5079 m). *Atmos. Chem. Phys.* **2010**, *10*, 7515–7531.
46. Government of Nepal, National Planning Commission Secretariat, Central Bureau of Statistics National Population and Housing Census 2011 (National Report). 2012. Available online: https://unstats.un.org/unsd/demographic-social/census/documents/Nepal/Nepal-Census-2011-Vol1.pdf (accessed on 18 September 2020).
47. Neupane, N.; Ramachandra Murthy, M.S.; Rasul, G.; Wahid, S.; Shrestha, A.B.; Uddin, K. Integrated Biophysical and Socioeconomic Model for Adaptation to Climate Change for Agriculture and Water in the Koshi Basin. In *Handbook of Climate Change Adaptation*; Springer: Berlin, Germany, 2013.
48. Sahas Urja. Solu Khola (Dudhkoshi) Hydro-Electric Project—86MW. Salient Features. 2018. Available online: http://sahasurja.com/project/solu-khola-dudhkoshi-hydro-electric-project-86mw/ (accessed on 18 September 2020).
49. Soncini, A.; Bocchiola, D.; Azzoni, R.S.; Diolaiuti, G. A methodology for monitoring and modeling of high altitude Alpine catchments. *Prog. Phys. Geogr.* **2017**, *41*, 393–420. [CrossRef]
50. Shea, J.M.; Immerzeel, W.W.; Wagnon, P.; Vincent, C.; Bajracharya, S. Modelling glacier change in the Everest region, Nepal Himalaya. *Cryosphere* **2015**, *9*, 1105–1128. [CrossRef]
51. Peel, M.C.; Finlayson, B.L.; McMahon, T.A. Updated world map of the Köppen-Geiger climate classification. *Hydrol. Earth Syst. Sci.* **2007**, *11*, 1633–1644. [CrossRef]
52. WWF, World Wildlife Fund, Nepal. *Water Poverty of Indrawati Basin, Analysis and Mapping, June 2012*; WWF: Kathmandu, Nepal, 2012. Available online: http://awsassets.panda.org/downloads/water_poverty_book.pdf (accessed on 18 September 2020).
53. Cook, S.; Rubiano, J.; Sullivan, C.; Andah, W.; Ashante, F.; Wallace, J.; Terrasson, I.; Nikiema, A.; Kemp-Benedict, E.; Tourino, I.; et al. Water poverty mapping in the Volta basin. In Proceedings of the CGIAR Challenge program on water and food, Workshop report, Accra, Ghana, 3–8 March 2007. Available online: http://cpwfbfp.pbworks.com/f/Water_poverty_mapping_Volta_Ghana_Workshop_Report.pdf (accessed on 18 September 2020).
54. NAPA. *National Adaptation Programme of Action (NAPA)*; Government of Nepal, Ministry of Environment: Kathmandu, Nepal, 2010.
55. ICIMOD. *Nepal's Digital Agriculture Atlas*; ICIMOD: Kathmandu, Nepal, 2015. Available online: http://geoportal.icimod.org/?q=21298 (accessed on 18 September 2020).
56. FAO. The Soil and Terrain database (SOTER) for Nepal. 2004. Available online: http://www.fao.org/soils-portal/soil-survey/soil-maps-and-databases/regional-and-national-soil-maps-and-databases/en/ (accessed on 18 September 2020).
57. Higuchi, K.; Ageta, Y.; Yasunari, T.; Inoue, J. Characteristics of precipitation during the monsoon season in high-mountain areas of the Nepal Himalaya. *Hydrol. Asp. Alp. High-Mt. Areas* **1982**, *138*, 21–30.
58. Salerno, F.; Guyennon, N.; Thakuri, S.; Viviano, G.; Romano, E.; Vuillermoz, E.; Cristofanelli, P.; Stocchi, P.; Agrillo, G.; Ma, Y.; et al. Weak precipitation, warm winters and springs impact glaciers of south slopes of Mt. Everest (central Himalaya) in the last 2 decades (1994–2013). *Cryosphere* **2015**, *9*, 1229–1247. [CrossRef]

59. Bocchiola, D. Use of Scale Recursive Estimation for multi-sensor rainfall assimilation: A case study using data from TRMM (PR and TMI) and NEXRAD. *Adv. Water Resour.* **2007**, *30*, 2354–2372. [CrossRef]
60. Bookhagen, B. High resolution spatiotemporal distribution of rainfall seasonality and extreme events based on a 12-year TRMM time series. 2012. Available online: http://www.geog.ucsb.edu/~{}bodo/pdf/bookhagen_global_TRMM_extremeE_DR_final.pdf (accessed on 18 September 2020).
61. Bocchiola, D.; Soncini, A.; Senese, A.; Diolaiuti, G. Modelling hydrological components of the Rio Maipo of Chile, and their prospective evolution under climate change. *Climate* **2018**, *6*, 57. [CrossRef]
62. OCHA, Office for the Coordination of Humanitarian Affairs, Nepal. 2015. Available online: https://www.unocha.org/asia-and-pacific-roap/nepal (accessed on 18 September 2020).
63. Worldpop. Open spatial demographic data. Available online: https://www.worldpop.org/.2015 (accessed on 18 September 2020).
64. Stevens, F.R.; Gaughan, A.E.; Linard, C.; Tatem, A.J. Disaggregating Census Data for Population Mapping Using Random Forests with Remotely-Sensed and Ancillary Data. *PLoS ONE* **2015**, *10*, e0107042. [CrossRef] [PubMed]
65. Siddaiah, R.; Saini, R.P. A review on planning, configurations, modeling and optimization techniques of hybrid renewable energy systems for off-grid applications. *Renew. Sustain. Energy Rev.* **2016**, *58*, 376–396. [CrossRef]
66. Soncini, A.; Bocchiola, D.; Confortola, G.; Bianchi, A.; Rosso, R.; Mayer, C.; Lambrecht, A.; Palazzi, E.; Smiraglia, C.; Diolaiuti, G. Future hydrological regimes in the Upper Indus basin: A case study from a high-altitude glacierized catchment. *J. Hydrometeorol.* **2015**, *16*, 306–326. [CrossRef]
67. Aili, T.; Soncini, A.; Bianchi, A.; Diolaiuti, G.; D'Agata, C.; Bocchiola, D. Assessing water resources under climate change in high-altitude catchments: A methodology and an application in the Italian Alps. *Appl. Clim.* **2018**, *135*, 1–22. [CrossRef]
68. Oerlemans, J. *Glaciers and Climate Change*; A.A. Balkema Publishers: Brookfield, VT, USA, 2001; p. 148.
69. Haeberli, W.; Hölzle, M. Application of inventory data for estimating characteristics of and regional climate-change effects on mountain glaciers: A pilot study with the European Alps. *Ann. Glaciol.* **1995**, *21*, 206–212. [CrossRef]
70. Rosso, R. Nash model relation to Horton order ratios. *Water Resour. Res.* **1984**, *20*, 914–920. [CrossRef]
71. Shrestha, S.; Khatiwada, M.; Babel, M.S.; Parajuli, K. Impact of Climate Change on River Flow and Hydropower Production in Kulekhani Hydropower Project of Nepal. *Environ. Process.* **2014**, *1*, 231–250. [CrossRef]
72. International Energy Agency IEA. *Nepal Energy Balance Flow*; IEA: Paris, France, 2015.
73. Proietti, S.; Sdringola, P.; Castellani, F.; Astolfi, D.; Vuillermoz, E. On the contribution of renewable energies for feeding a high altitude Smart Mini Grid. *Appl. Energy* **2017**, *185*, 15–20. [CrossRef]
74. Salerno, F.; Viviano, G.; Mangredi, E.C.; Caroli, P.; Thakuri, S.; Tartari, G. Multiple Carrying Capacities from a management-oriented perspective to operationalize sustainable tourism in protected area. *J. Environ. Manag.* **2013**, *128*, 116–125. [CrossRef]
75. ICIMOD. *Regional Data Base Initiative*; ICIMOD: Kathmandu, Nepal, 2017. Available online: http://www.icimod.org/?q=rdi (accessed on 18 September 2020).
76. Ogayar, B.; Vidal, P.G. Cost determination of the electro-mechanical equipment of a small hydro-power plant. *Renew. Energy* **2009**, *34*, 6–13. [CrossRef]
77. Silver, E. An overview of heuristic solution methods. *J. Oper. Res. Soc.* **2004**, *55*, 936–956. [CrossRef]
78. Ranaboldo, M.; Ferrer Martì, L.; Garcia-Villoria, A.; Moreno, R.P. Heuristic indicators for the design of community off-grid electrification systems based on multiple renewable energies. *Energy* **2013**, *50*, 501–512. [CrossRef]
79. Ranaboldo, M.; Garcia-Villoria, A.; Ferrer-Martì, L.; Moreno, R.P. A heuristic method to design autonomous village electrification projects with renewable energies. *Energy* **2014**, *73*, 96–109. [CrossRef]
80. Ranaboldo, M.; Garcia-Villoria, A.; Ferrer-Martì, L.; Moreno, R.P. A meta-heuristic method to design off-grid community electrification projects with renewable energies. *Energy* **2015**, *93*, 2467–2482. [CrossRef]
81. Groppelli, B.; Soncini, A.; Bocchiola, D.; Rosso, R. Evaluation of future hydrological cycle under climate change scenarios in a mesoscale Alpine watershed of Italy. *Nat. Haz. Earth Sys. Sci.* **2011**, *11*, 1769–1785. [CrossRef]

82. Stevens, B.; Giorgetta, M.; Esch, M.; Mauritsen, T.; Crueger, T.; Rast, S.; Salzmann, M.; Schmidt, H.; Bader, J.; Block, K.; et al. Atmospheric component of the MPI-M Earth System Model: ECHAM6. *J. Adv. Model. Earth Syst.* **2013**, *5*, 1–27. [CrossRef]
83. Gent, P.R.; Danabasoglu, G.; Donner, L.J.; Holland, M.M.; Hunke, E.C.; Jayne, S.R.; Lawrence, D.M.; Neale, R.B.; Rasch, P.J.; Vertenstein, M.; et al. The Community Climate System Model Version 4. *J. Clim.* **2011**, *24*, 4973–4991. [CrossRef]
84. Hazeleger, W.; Wang, X.; Severijns, C.; Ştefănescu, S.; Bintanja, R.; Sterl, A.; Wyser, K.; Semmler, T.; Yang, S.; van den Hurk, B.; et al. EC-Earth V2.2: Description and validation of a new seamless earth system prediction model. *Clim. Dyn. J.* **2011**, *39*, 2611–2629. [CrossRef]
85. Savéan, M.; Delclaux, F.; Chevallier, P.; Wagnon, P.; Gonga-Saholiariliva, N.; Sharma, R.; Neppel, L.; Arnaud, Y. Water budget on the Dudh Koshi River (Nepal): Uncertainties on precipitation. *J. Hydrol.* **2015**, *531*, 850–862. [CrossRef]
86. Manara, M. Planning rural electrification with mini hydro-power systems in the Dudh Koshi basin (Nepal). Master's Thesis, Politecnico di Milano, Milan, Italy, 2018.
87. Bolch, T.; Shea, J.M.; Liu, S.; Azam, F.M.; Gao, Y.; Gruber, S.; Immerzeel, W.W.; Kulkarni, A.; Li, H.; Tahir, A.A.; et al. Status and change of the cryosphere. In *The Hindu Kush Himalaya Assessment*; Wester, P., Mishra, A., Mukherji, A., Shrestha, A.B., Eds.; Springer: Cham, Switzerland, 2019; pp. 209–255.
88. Pathak, M. Climate Change: Uncertainty for Hydropower Development in Nepal. *Hydro Nepal* **2010**, *6*, 31–34. [CrossRef]
89. Bombelli, G.M.; Soncini, A.; Bianchi, A.; Bocchiola, D. Potentially modified hydropower production under climate change in the Italian Alps. *Hydrol. Process* **2019**. [CrossRef]
90. Butler, C.; Rest, M. Calculating Risk, Denying Uncertainty: Seismicity and Hydropower Development in Nepal. *Himalaya* **2017**, *37*, 15–25.
91. Huber, H. Hydropower in the Himalayan Hazardscape: Strategic Ignorance and the Production of Unequal Risk. *Water* **2019**, *11*, 414. [CrossRef]